

RESEARCH

Open Access



Outcomes of gamma knife treated large symptomatic arteriovenous malformations according to guidelines of Taiwan neurosurgical consensus

Ming-Hsi Sun^{1†}, Yuang-Seng Tsuei¹, Ting-Wei Wang², Szu-Yuan Liu¹, Ying Ju Chen³, Chiung-Chyi Shen¹, Meng-Yin Yang¹, Jason Sheehan⁴, Weir-Chiang You^{5†}, Meei-Ling Sheu^{6,7,8} and Hung-Chuan Pan^{1,7,8*}

Abstract

Background The treatment of large arteriovenous malformations (AVMs), in particular those unruptured, remains a topic of debate. Stereotactic radiosurgery has favorable outcomes for small to medium-sized AVMs. However, for large AVMs, the goal is to maximize obliteration rates and at the same time, to minimize radiation-induced complications. This study assessed outcomes of large symptomatic AVMs treated with Gamma Knife radiosurgery (GKRS) focusing on cases presenting with rupture or seizures. The study followed the guidelines of Taiwan Neurosurgical Consensus, a government-funded committee under the Central Bureau of Health Insurance that determines whether radiosurgery is an appropriate treatment.

Materials and methods This retrospective study included 75 cases of large AVMs (> 10 cc) treated with GKRS during the period from June 2003 to January 2020. Inclusion criteria were as follows: a history of intracerebral hemorrhage (ICH) or seizures, no prior embolization, and periodic MRI examinations with clinical assessments post-GKRS. Treatment procedures were adapted based on the Taiwan Neurosurgical Consensus guidelines.

Results The average patient age was 36.4 ± 16.1 years, with a median follow-up duration of 104 (range 82–150) months. Forty-six patients (61.3%) underwent single-stage treatment, while 29 patients (38.7%) received two-stage treatment. The mean AVM volume was 20.5 ± 11.7 cc, with an average peripheral radiation dose of 17.7 ± 1.2 Gy. Among the 32 cases with AVM volumes between 10 and 15 cc, 25 (78.1%) achieved total obliteration. For the 17 cases with volumes between 15 and 20 cc, 7 (41.2%) achieved total obliteration, while 8 out of 26 (30.8%) cases with volumes > 20 cc achieved total obliteration. Severe brain edema developed in 16 patients (21.3%) after an average follow-up of 105.4 ± 56.2 months, but 11 patients (14.6%) experienced symptoms. Only one patient (1.3%) suffered neurological disability. Seizure control in Engel classification I was achieved in 21 of 42 patients (50%). Eight patients (10.6%) experienced new hemorrhages, with 4 (12.1%) occurring in those with a prior history of hemorrhage (annual

[†]Ming-Hsi Sun and Weir-Chiang You contributed equally to this work.

*Correspondence:
Hung-Chuan Pan
hcpan2003@yahoo.com.tw

Full list of author information is available at the end of the article



© The Author(s) 2025. **Open Access** This article is licensed under a Creative Commons Attribution-NonCommercial-NoDerivatives 4.0 International License, which permits any non-commercial use, sharing, distribution and reproduction in any medium or format, as long as you give appropriate credit to the original author(s) and the source, provide a link to the Creative Commons licence, and indicate if you modified the licensed material. You do not have permission under this licence to share adapted material derived from this article or parts of it. The images or other third party material in this article are included in the article's Creative Commons licence, unless indicated otherwise in a credit line to the material. If material is not included in the article's Creative Commons licence and your intended use is not permitted by statutory regulation or exceeds the permitted use, you will need to obtain permission directly from the copyright holder. To view a copy of this licence, visit <http://creativecommons.org/licenses/by-nc-nd/4.0/>.

bleeding rate: 1.2%) and 4 (9.5%) in those patients with a history of seizures (annual bleeding rate: 1.1%). Univariate analyses showed that total obliteration was significantly associated with smaller nidus volumes (< 15 cc), single-stage radiosurgery, Radiosurgery-Based Grading Scale, first-stage volume, maximum dose, 12 Gy volume, and nidus coverage percentages at 16 Gy and 18 Gy. Multivariate analyses revealed that post-GKRS symptoms and severe brain edema were significantly correlated with the following: Virginia Radiosurgery AVM Score, Charlson Comorbidity Index, and mean radiation dose.

Conclusion The obliteration rate of large AVMs is strongly correlated with their size. This approach appears to achieve the goals of obliteration and minimizing the risks of radiation-induced complications and hemorrhage. Further investigation is needed for adjuvant treatments in residual or refractory cases after GKRS.

Keywords Large arteriovenous malformation, Stereotactic radiosurgery, Volume-stage

Introduction

Cerebral arteriovenous malformations (AVMs) are rare but complex vascular lesions. For patients, they present significant risks, like hemorrhage, seizures, and other neurological complications. The estimated annual rupture rate for AVMs is 2 to 4%, with the risk of hemorrhage varies depending on factors such as AVM location and venous drainage. Unruptured AVMs at superficial locations have a hemorrhage rate of less than 1%, while ruptured, deep-seated AVMs can have a rate as high as 33% [1–3]. Hemorrhages from AVMs are associated with a 50% chance of a new neurological deficit and a 10% fatality rate [4, 5]. These statistics emphasize the critical importance of proper treatment for AVM patients, particularly for those with rupture.

One pivotal study on AVM management, the ARUBA trial, emphasized the potential benefits of conservative treatment for patients with unruptured AVMs. This was a multicenter, prospective, randomized trial involving 223 patients assigned to one of two groups: medical therapy alone and medical treatment combined with interventional treatment. The trial was prematurely halted after findings indicated that medical therapy alone was more effective in preventing death or stroke [6]. Similarly, a prospective cohort study by Al-Shahi Salman et al., in which 204 patients with unruptured AVMs were followed over a median of 6.9 years, concluded that patients managed conservatively had better clinical outcomes [7]. Despite these findings, the use of interventional treatment for unruptured AVMs remains debated, particularly in terms of its potential to prevent future hemorrhage and associated complications.

Seizure is the second most common manifestation of AVMs, occurring in 11 to 35% of cases [8–12]. Several factors contribute to their risk of seizures, including male gender, young age, AVM location in the frontal or temporal lobes, as well as large AVMs (> 3 cm) [9, 13, 14]. While treatment for AVM-related seizures has been the subject of debate, interventions like microsurgical resection and stereotactic radiosurgery (SRS) have shown promise. For patients with drug-resistant epilepsy (DRE),

microsurgical resection often results in poor outcomes [15]. In contrast, SRS is more successful in reducing seizure activity, with favorable outcomes in as many as 80% of cases [16]. These suggest that treating AVMs harboring the symptoms of seizure with stereotactic radiosurgery is a reasonable approach.

Treating large AVMs (defined as those greater than 3 cm in diameter, or 10 cm³ in volume), presents unique challenges. Single-session stereotactic radiosurgery (SS-SRS) is typically less effective for large AVMs, as higher radiation doses are required for obliteration, leading to greater risk of adverse effects such as radiation edema or necrosis [17–19]. Volume-staged stereotactic radiosurgery (VS-SRS) has emerged as a promising alternative, by dividing the AVM into smaller, and more treatable portions. This approach allows the application of higher doses while minimizing complications, despite the difficulty in a complete obliteration based on VS-SRS alone [20, 21]. VS-SRS could transform previously inoperable, high-grade AVMs into more operable AVMs by reducing the lesion size and risk profile. This approach is more beneficial for young patients with a longer life expectancy and higher hemorrhage risks [22]. For optimal outcome, other detail related to AVM size needed to be considered in order to reach a balance the efficacy of radiation response and potential complications.

Spetzler-Martin grading scale was developed 38 years ago to predict outcomes after AVM resection [23]. Prediction accuracy of this scale has been questioned, in particular for large AVMs treated with radiosurgery [24]. While the scale is useful for surgical patients, the Radiosurgery-Based Grading Scale (RBAS) and the Virginia Radiosurgery AVM Scale (VRAS) are alternative predictive tools for patients undergoing stereotactic radiosurgery. These two later scales focus on variables such as AVM volume, patient age, and AVM location measured in points or continuous scales, yielding more accurate predictions for radiosurgical cases [19, 25]. The Charlson Comorbidity Index (CCI) is a method used to predict mortality by classifying or weighting comorbid conditions [26]. While the CCI is widely utilized across

various medical fields to assess patient risk profiles, its direct application in predicting outcomes for large AVMs treated with GKRS remains unclear [27]. However, evaluating a patient’s overall health status using tools like the CCI can be essential when considering treatment options, as higher comorbidity scores may influence both treatment decisions and potential outcomes.

In Taiwan, a neurosurgical consensus has established guidelines for the treatment of large AVMs, restricting the volume treated in a single session to 20 cc. The Taiwan Neurosurgical Consensus, a government-funded committee under the Central Bureau of Health Insurance, is responsible for determining whether radiosurgery is an appropriate treatment option. Cases exceeding this volume require double-blind approval. Accordingly, our treatment protocol has been modified: AVMs smaller than 15 cc are treated in a single session; AVMs between 15 and 20 cc are treated in either one or two stages, depending on eloquence; and AVMs larger than 20 cc are treated in two stages. This approach aims to reach a balance between maximizing the obliteration rates and minimizing radiation-induced complications. Here, we assessed the effectiveness of this treatment strategy in term of obliteration rates, neurological outcomes, imaging changes, and seizure control, with special attention given to the influence of AVM grade on radiosurgery outcomes.

Materials and methods

Patient population

In this retrospective study, which had been approved by our institutional review board, we reviewed all AVM patients treated with Gamma Knife radiosurgery (GKRS) at our institute between June 2003 and January 2020. Inclusion criteria were the following: AVM > 10 cc, history of intracerebral hemorrhage (ICH) or seizures, no

prior embolization, and receiving periodic MRI exams with post GKRS clinical assessments.

In Taiwan, and AVMs > 20 cc or with a maximum diameter > 3.5 cm is considered worrisome for poor outcomes after stereotactic radiosurgery, as per the consensus of the Taiwan Neurosurgical Society. The Taiwan Neurosurgical Consensus, a government-funded committee under the Central Bureau of Health Insurance, is responsible for determining whether radiosurgery is an appropriate treatment option. Under this guideline, our treatment algorithm for large AVMs (Fig. 1) was as follows: AVMs > 20 cc is treated in two stages (Fig. 2); 15 to 20 cc in eloquent locations are treated in two stages (Fig. 3); 15–20 cc in non-eloquent locations in a single stage (Fig. 4); and AVMs < 15 cc in a single stage (Fig. 5). Eloquent locations include the basal ganglia, thalamus, brainstem, or functional areas involved in vision, speech, sensorimotor function, and hearing.

At the follow-up of each patient, we performed the following: neurological assessments, MRI, and angiography (when MRI has indicated obliteration). A total of 80 patients with large AVMs were identified. Two patients declined angiography, and three were excluded due to lack of regular follow-up. Thus, 75 cases were finally analyzed.

Radiosurgical technique

After administering local anesthesia, the Leksell G head frame was attached, and the patient was monitored for blood pressure and oxygenation, together with electrocardiography. For radiosurgical targeting and planning, we used the high-resolution biplanar and stereotactic cerebral angiography. Selective injections were applied as needed into the vertebral, internal carotid (ICA), or external carotid arteries (ECA). The AVM nidus was localized with MRI and MR angiography, including

The algorithm of large AVM treated by GK

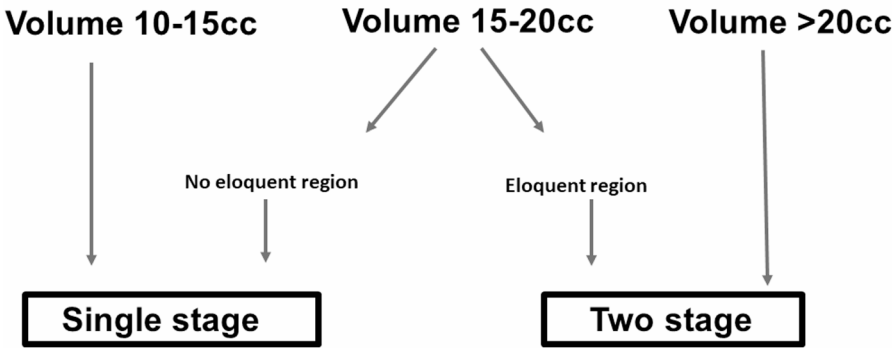


Fig. 1 Gamma knife treatment algorithm. AVMs > 20 cc are treated in two stages; 15–20 cc in eloquent locations are treated in two stages; 15–20 cc in non-eloquent locations in a single stage; and AVMs < 15 cc in a single stage

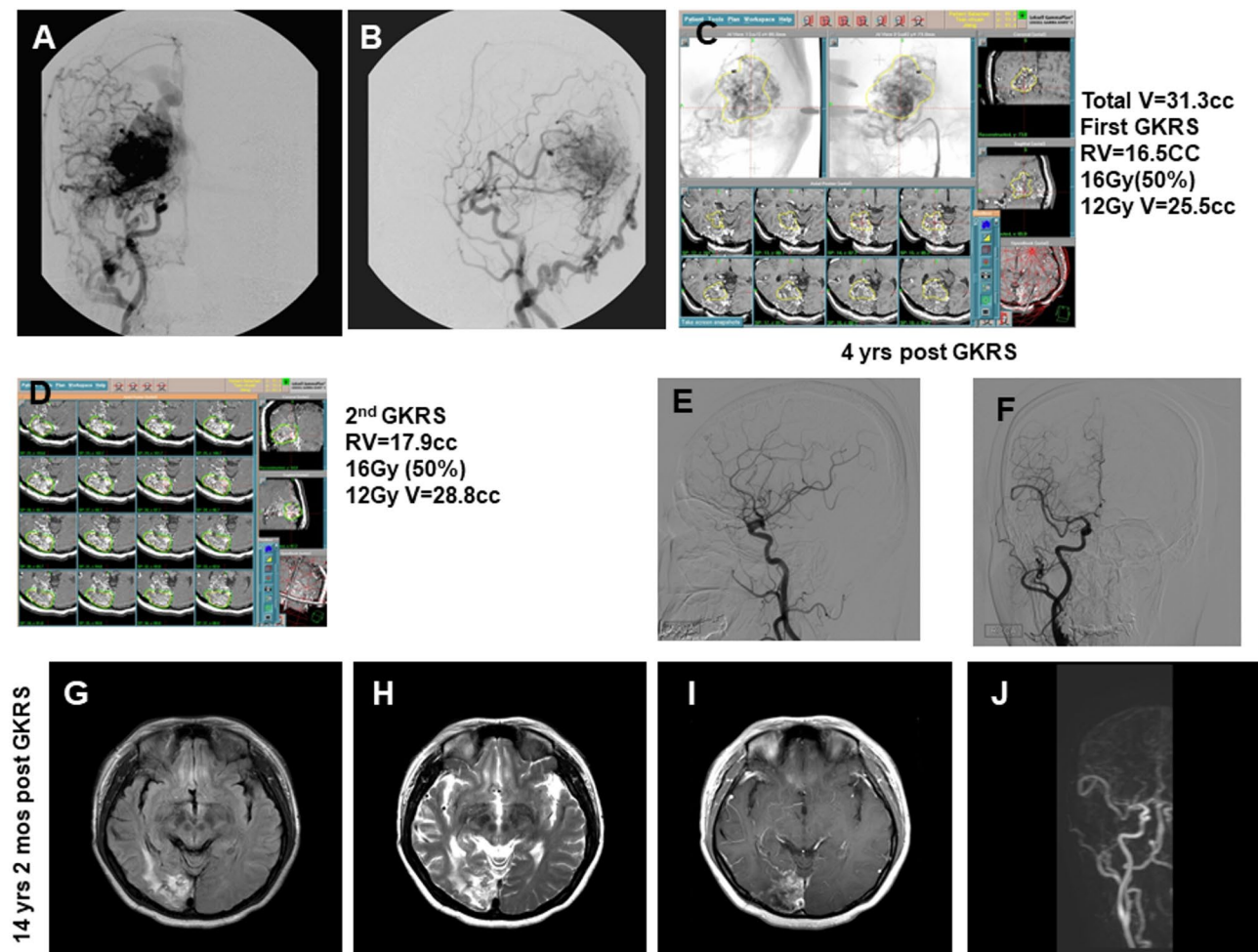


Fig. 2 A 35-year-old female with the focal seizure and diagnosed as a huge AVM with volume of 31 cc under the guidance of AVM volume > 20 cc treated in two stage gamma knife treatment. The post GKRS imaging showed total obliteration without any neurological deficits. **(A)** Anteroposterior view of cerebral angiography following right common carotid contrast injection showed a large AVM located in the occipital lobe. The AVM was supplied by branches from the right external carotid artery and internal cerebral artery, with venous drainage into the straight, transverse, and superior sagittal sinuses. **(B)** Lateral view of cerebral angiography after right common carotid contrast injection demonstrated a large AVM in the occipital lobe, with arterial supply from the right external carotid artery and internal cerebral artery. Venous drainage was observed into the straight, transverse, and superior sagittal sinuses. **(C)** Photograph illustrating dose planning for the first stage of Gamma Knife radiosurgery (GKRS). Treatment parameters are shown on the right side of the image. The yellow line indicates the 50% isodose line. **(D)** Photograph showing dose planning for the second stage of GKRS. Treatment parameters are displayed on the right side of the image. The yellow line represents the 50% isodose line. **(E)** No definite nidus was observed in the lateral view of cerebral angiography 4 years after GKRS. **(F)** No definite nidus was noted in the anteroposterior view of cerebral angiography 4 years after GKRS. **(G)** A small residual abnormality in the right occipital region was detected on FLAIR sequence imaging 14 years and 2 months after GKRS. **(H)** Small residual abnormalities in the right occipital region were observed on T2-weighted MRI 14 years and 2 months after GKRS. **(I)** Mild residual contrast enhancement was seen in the right occipital region on T1-weighted MRI with contrast. **(J)** No definite nidus was detected on MRA 14 years and 2 months after GKRS

T1-weighted, T2-weighted, time-of-flight (TOF), spoiled gradient recall, and Gd-enhanced sequences. Images were transferred to the Leksell GammaPlan station (Elekta Instruments AB), where the target was delineated using fused MRI and angiography.

Radiosurgery dose plans, using single or multiple isocenters, were generated to cover the target contour. All patients received a margin dose of 16 to 20 Gy, prescribed to the 40–60% isodose line, delivered with the Leksell Gamma Knife Model D (Elekta AB). A four-member team, including a neurosurgeon, neuroradiologist,

radiation oncologist, and medical physicist, oversaw the treatment process. From these patients, 46 lesions were treated in a single session, and 29 in two stages, with intervals of 3 to 6 months. The AVM nidus was divided into grossly equal portions using cross-sectional MRI.

We divided the volume of the arteriovenous malformation (AVM) into two parts using a superior/inferior division based on a series of axial cuts from TOF MRA. These two parts were divided as equally as possible in volume, with a recognized anatomical landmark serving as a reference for the next treatment section. The inferior

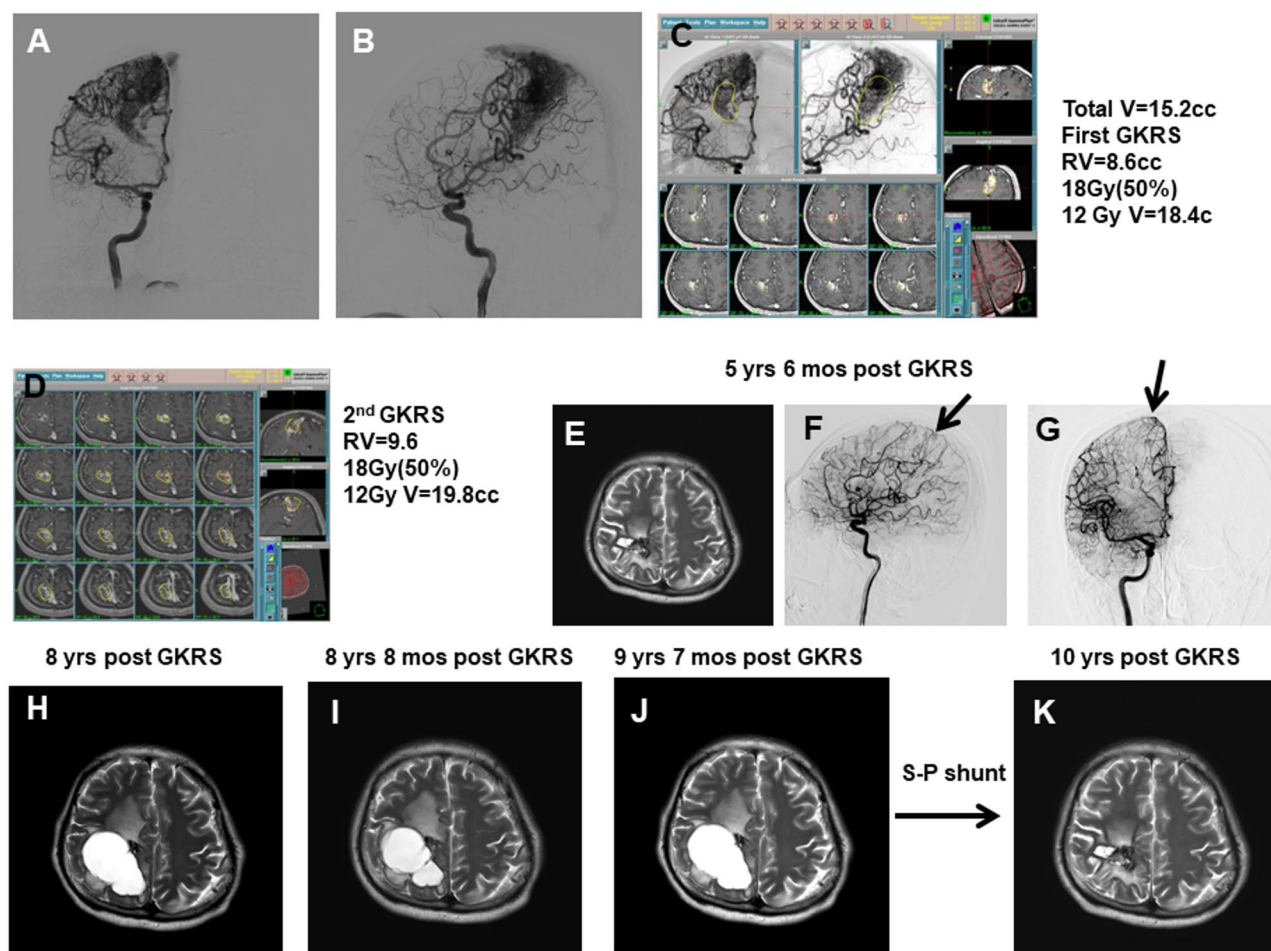


Fig. 3 A 28-year-old male presented with focal seizure and diagnosed as a huge AVM with volume of 15.2 cc. The treatment was separated into 2 stages under the guidance of AVM volume 15–20 cc in eloquent locations treated in two stages treatment. The post GKRS imaging showed the tiny residual nidus and cyst formation mandatory of s-p shunt with clinical symptoms of left leg clumsy movement. **(A)** Anteroposterior view of cerebral angiography showed an AVM located in the right parietal lobe, with arterial supply from the right anterior and middle cerebral arteries and venous drainage into the deep venous system and the superior sagittal sinus. **(B)** Lateral view of cerebral angiography showed an AVM in the right parietal lobe, supplied by the right anterior and middle cerebral arteries, with drainage into the deep venous system and the superior sagittal sinus. **(C)** Photograph showing dose planning for the first stage of Gamma Knife radiosurgery. Treatment parameters are displayed on the right side of the image. The yellow line represents the 50% isodose line. **(D)** Photograph showing dose planning for the second stage of Gamma Knife radiosurgery. Treatment parameters are shown on the right side of the image. The yellow line indicates the 50% isodose line. **(E)** A small cyst was detected at the targeted lesion on T2-weighted MRI, 5 years and 6 months after the first GKRS. However, no definite symptoms were noted at that time. **(F)** A small nidus, indicated by the arrowhead, was identified in the lateral view of cerebral angiography 5 years and 6 months after the first GKRS. **(G)** A small nidus, indicated by the arrowhead, was detected in the anteroposterior view of cerebral angiography 5 years and 6 months after the first GKRS. **(H)** A large cyst in the right parietal region was observed on T2-weighted MRI 5 years and 9 months after GKRS. Neurological examination revealed clumsiness in the left leg. **(I)** A large cyst in the right parietal region was noted on T2-weighted MRI 6 years and 3 months after GKRS. Neurological examination showed continued clumsiness in the left leg without further deterioration. **(J)** A large cyst in the right parietal region was detected on T2-weighted MRI 7 years and 3 months after Gamma Knife treatment. Neurological examination revealed worsening clumsiness in the left leg. A cyst-peritoneal shunt was scheduled at this time. **(K)** A small residual cyst was detected on T2-weighted MRI 10 months after the cyst-peritoneal shunt. Neurological examination showed improvement in left leg movement

part of the nidus was treated first, followed by the superior part, with an interval of 3 to 6 months between radiosurgical procedures.

Parameters of gamma knife treatment

The grading systems we had used included the following: Spetzler-Martin grading scale [23], Radiosurgery-Based Grading Scale [19], Virginia Radiosurgery AVM

Scale [25], and Charlson Comorbidity Index [27]. These data were calculated and then correlated with both imaging and clinical outcomes. The radiosurgery parameters included margin dose, maximum dose, mean dose, 12 Gy volume, and the percentage of the target volume covered at 16 Gy, 18 Gy, and 20 Gy. Angiographic characteristics, such as the number of feeding arteries and the number

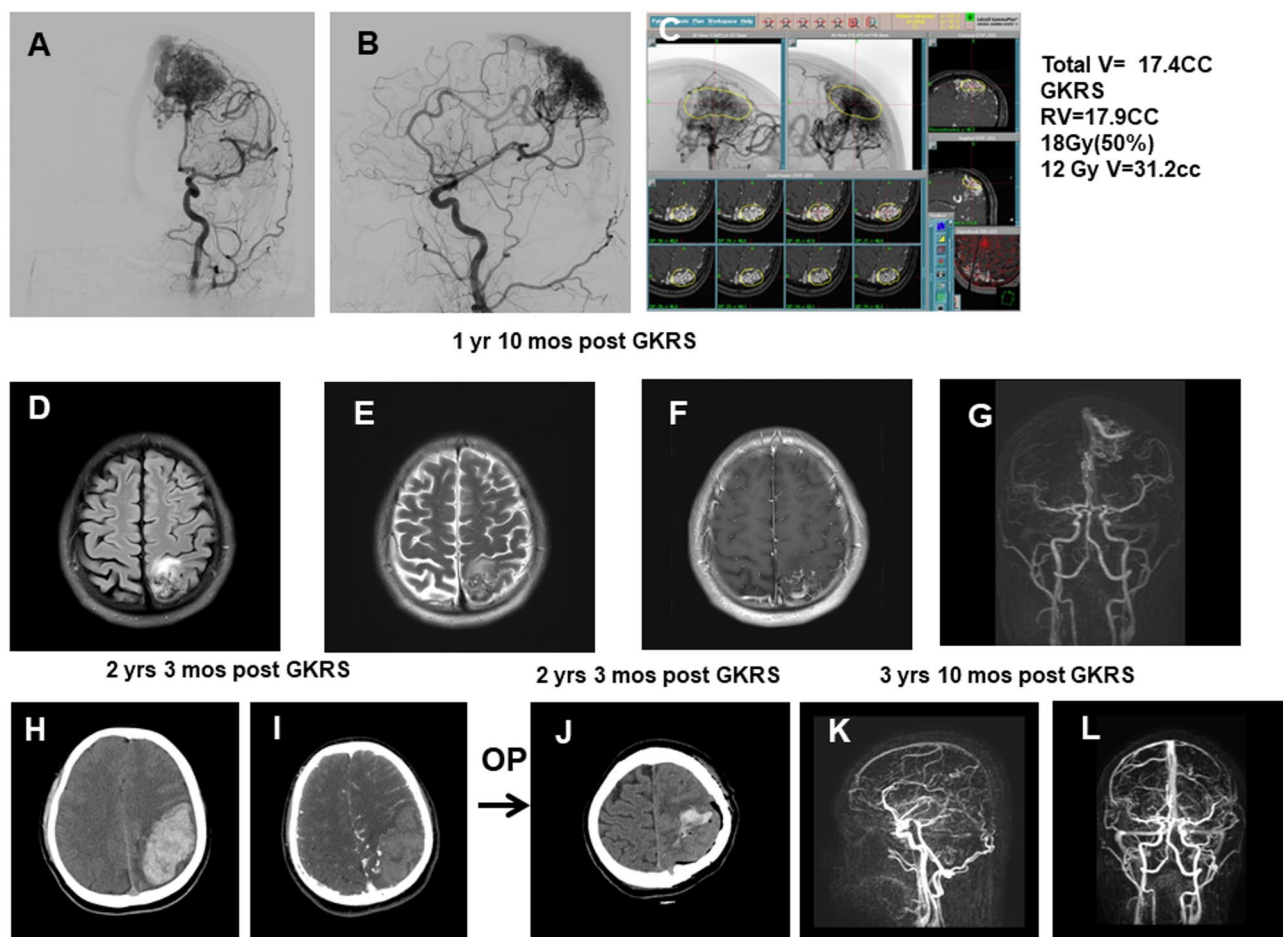


Fig. 4 A 23-year-old male presented with focal seizure and diagnosed as huge AVM with volume of 17.4 cc. The treatment was conducted in a single stage according to the guidance of AM volume 15–20 cc in no-eloquent locations treated in single stage. The patient suffered severe headache after Gamma Knife radiosurgery due to the hemorrhage and received the craniotomy for hematoma removal. The patient gained full recovery without neurological deficits with Engle I of seizure control. **(A)** A large AVM located in the left parietal lobe was detected in the anteroposterior view of cerebral angiography, with arterial supply from the anterior cerebral artery and venous drainage into the superior sagittal sinus. **(B)** A large AVM in the left parietal lobe was observed in the lateral view of cerebral angiography, with feeding arteries from the anterior cerebral artery and drainage into the superior sagittal sinus. **(C)** Photograph showing dose planning for Gamma Knife radiosurgery (GKRS). Treatment parameters are displayed on the right side of the image. The yellow line indicates the 50% isodose line. **(D)** A small abnormal signal in the left parietal region was observed on FLAIR imaging one year and 10 months after GKRS. **(E)** A small abnormal signal was detected in the left parietal region on T2-weighted MRI one year and 10 months after GKRS. **(F)** Mild abnormal enhancement resembling a vascular structure was seen in the left parietal region one year and 10 months after GKRS. **(G)** A small nidus with early draining veins in the left parietal region was detected on MRA one year and 10 months after GKRS. **(H)** The patient experienced a severe headache and was diagnosed with intracerebral hemorrhage in the left parietal region by CT scan 2 years and 3 months after GKRS. **(I)** A small abnormal vascular structure in the left parietal region was identified by CTA 2 years and 3 months after GKRS. **(J)** A small residual intracerebral hemorrhage at the surgical bed was seen on brain CT the day after surgery. Neurological examination revealed no definite deficits. **(K)** No definite nidus was observed in the lateral view of MRA 3 years and 10 months after GKRS. **(L)** No definite nidus was seen in the anteroposterior view of MRA 3 years and 10 months after GKRS

and location of drainage veins, were also reviewed and correlated with the outcomes.

Clinical and imaging Follow-Up

Patients were followed up in neurosurgical outpatient clinics at intervals of 2 to 3 months during the first year after GKRS, followed by annual visits thereafter. Clinical data collected at each follow-up included detailed neurological examinations and assessment of seizure status according to Engel classification.

Follow-up MRI scans were performed 3 to 6 months after GKRS, then at intervals of 6 to 12 months, and later at one- to two-year intervals. MRI sessions included T1-weighted, T2-weighted, time of flight (TOF), and gadolinium-enhanced sequences, and results were compared with pretreatment images. MRI data were used to evaluate nidus obliteration and to identify any unintended postoperative effects visible on images.

For patients whose MRI showed complete obliteration, additional angiography was performed. All images were

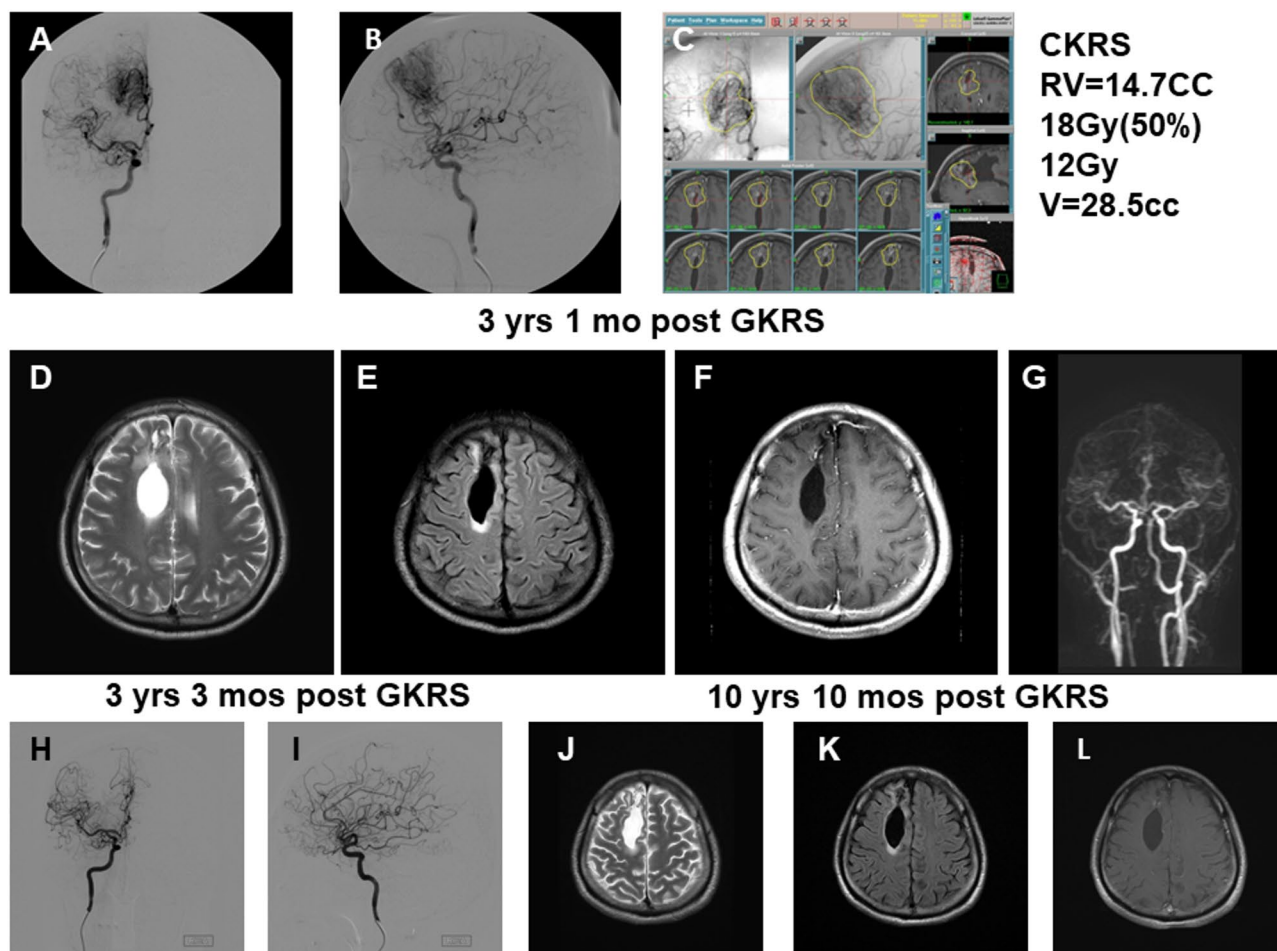


Fig. 5 A 39-year-old male presented with right frontal hemorrhage and diagnosed as a huge AVM with volume of 14.7 cc. The treatment was conducted in single stage treatment according to the guidance of AVM volume 10–15 cc procedure in single stage. The post GKRS angiography showed the total obliteration after gamma knife and MRI showed a small cyst over the previous hemorrhage cavity. **(A)** A large right frontal AVM was detected in the anteroposterior view of cerebral angiography, with arterial supply from the anterior cerebral artery and venous drainage into the superior sagittal sinus. **(B)** A large right frontal AVM was observed in the lateral view of cerebral angiography, with feeding arteries from the anterior cerebral artery and drainage into the superior sagittal sinus. **(C)** Photograph showing dose planning for Gamma Knife radiosurgery (GKRS). Treatment parameters are displayed on the right side of the image. The yellow line indicates the 50% isodose line. **(D)** A small abnormal signal surrounding the cyst cavity in the right frontal region was observed on T2-weighted MRI 3 years and 1 month after GKRS. **(E)** A small abnormal signal surrounding the cyst cavity in the right frontal region was seen on FLAIR imaging 3 years and 1 month after GKRS. **(F)** Mild abnormal enhancement resembling a vascular structure was noted in the right frontal region on contrast-enhanced T1-weighted MRI 3 years and 1 month after GKRS. **(G)** A small nidus with early venous drainage in the right frontal region was detected on MRA 3 years and 1 month after GKRS. **(H)** Cerebral angiography in the anteroposterior view showed no definite nidus 3 years and 3 months after GKRS. **(I)** Cerebral angiography in the lateral view revealed no definite nidus 3 years and 3 months after GKRS. **(J)** A small cyst without progression was observed in the right frontal region on T2-weighted MRI 10 years and 10 months after GKRS. **(K)** A small cyst without progression was also observed on FLAIR imaging 10 years and 10 months after GKRS. **(L)** No definite abnormal enhancement surrounding the cavity was seen 10 years and 10 months after GKRS. Neurological examination revealed no definite neurological deficits

reviewed by a neuroradiologist, using standard criteria [28, 29].

Statistical analyses

Descriptive statistics were reported using standard measures, such as mean \pm standard deviation, or median values and ranges. Factors contributing to cyst formation, post-GKRS intracerebral hemorrhage (ICH), patient death, and seizure freedom were assessed using the Mann–Whitney test, chi-square test, and Fisher's exact

test. Logistic regression analysis was employed to evaluate the total obliteration on angiograms, while the Cox regression test was used to determine risk factors associated with post GKRS symptoms, and severe brain edema on MRI. Statistical significance was set at p -value < 0.05 .

Results

Demographic data

The demographic data of the patients are presented in Table 1. The median age of patients was 36 (range 24–47)

Table 1 Patients demographics

	Total(<i>n</i> = 75)	Groups		<i>P</i> value
		Hemorrhage(<i>n</i> = 33)	Seizure(<i>n</i> = 42)	
Age (years)	36(24–47)	37(20–53)	25(24–43)	0.64
Male/Female	43/32	19/14	24/18	0.97
Neurological deficits	18(24%)	13(39.4%)	5(11.9%)	0.006
Previous operation	5(6.7%)	5(15.1%)	0	0.23
Follow up (months)	104(82–150)	112(81–159)	100(82–139)	0.28
Total volume	20.4 ± 11.7	16.4 ± 4.8	23.5 ± 14.4	0.63
Volume				0.008
Volume 10–15 cc	32(42.7%)	15(45.5%)	17(40.5%)	
Volume 15–20 cc	27(22.7%)	12(36.4%)	5(11.9%)	
Volume > 20 cc	26(34.7%)	6(18.2%)	20(47.6%)	
Treatment Stage				0.023
Single stage	46(61.3%)	25(75.8%)	21(50%)	
Two stages	29(38.7%)	8(24.2%)	21(50%)	
Location				0.228
Frontal/Temporal	25(33.3%)	12(36.4%)	13(31%)	
Parietal/occipital/corpus callosum/cerebellum	41(54.7%)	15(45.5%)	26(61.9%)	
Basal ganglia/thalamus /Brain stem	9(12%)	6(18.2%)	3(7.1%)	
Charlson comorbidity index	0.6 ± 1.2	0.8 ± 1.2	0.4 ± 1.2	0.16
Spetzler Martin grading	3.3 ± 0.6	3.2 ± 0.7	3.4 ± 0.5	0.26
Radiosurgery-Based Grading Scale	3.0 ± 1.2	2.6 ± 0.6	3.3 ± 1.4	0.1
Virginia Radiosurgery AVM Scale	3.1 ± 0.7	3.3 ± 0.7	2.9 ± 0.5	0.07
Number of feeding artery	1.7 ± 0.8	1.8 ± 0.9	1.7 ± 0.8	0.613
Number of drainage veins	1.3 ± 0.5	1.3 ± 0.5	1.3 ± 0.5	0.74
Number of Deep vein drainage	0.5 ± 0.6	0.6 ± 0.6	0.6 ± 0.4	0.25

Data was presented as mean ± standard deviation

years, with a male-to-female ratio of 43:32. Thirty-three patients had a history of intracerebral hemorrhage, and 42 had a history of seizures. The mean nidus volume was 20.5 ± 11.7 cc, with 16.5 ± 4.8 cc for patients with a history of hemorrhage and 23.5 ± 14.1 cc for those with a history of seizures. Nidus locations were distributed as follows: frontal/temporal lobe ($n = 25$, 33.3%), parietal/occipital/corpus callosum/cerebellum ($n = 41$, 54.7%), and basal ganglia/thalamus/brainstem ($n = 9$, 12.0%).

A total of 46 patients (61.3%) underwent single-stage radiosurgery, while 29 patients (38.7%) underwent two-stage treatment. Their mean Spetzler-Martin grading scale was 3.3 ± 0.6 , mean Radiosurgery-Based Grading Scale was 3 ± 0.6 , and the mean Virginia Radiosurgery AVM Scale was 3.1 ± 0.7 . Their mean Charlson Comorbidity Index was 0.6 ± 1.2 . Eighteen patients (24%) had neurological deficits prior to GKRS. Their mean number of feeding arteries was 1.7 ± 0.8 , while the mean number of draining veins was 1.3 ± 0.5 , with 0.5 ± 0.6 located in the deep venous drainage system.

Gamma knife radiosurgery parameters

The Gamma Knife radiosurgical parameters are displayed in Table 2. The mean peripheral dose was 17.7 ± 1.2 Gy, with a corresponding isodose line of $49.9 \pm 3.3\%$. The

mean radiation dose was 22.6 ± 1.1 Gy. The mean nidus coverage at 20 Gy, 18 Gy, and 16 Gy was $81.3 \pm 9.9\%$, $91.3 \pm 6.2\%$, and $97.6 \pm 3.5\%$, respectively. The mean volume at the 12 Gy isodose line was 37.9 ± 21.3 cc. For patients who underwent staged treatment, the mean volume of the first stage was 14.8 ± 4.6 cc, and the second stage was 15.4 ± 6.1 cc. The average interval between the first and second stages was 4.8 ± 1.5 months.

Treatment outcome

Clinical outcome

The treatment outcomes are detailed in Table 3. Eleven patients developed post GK symptoms, occurring at a median follow-up of 100 (79–150) months. Post-GKRS symptomatic patients included one individual experiencing clumsy leg movements with permanent neurological deficits. Three patients presented with increased seizure frequency, while seven suffered from severe headaches. All these patients required hospitalization. Three patients died: two from repeated hemorrhages and one from intractable seizures. In the seizure group ($n = 42$), 21 patients (50%) achieved seizure control classified as Engel I, 20 patients (47.6%) as Engel II, and one patient (2.3%) as Engel III.

Table 2 Parameters of GKRS

	Total (n = 75)	Groups		P value
		Hemorrhage(n = 33)	Seizure(n = 42)	
Peripheral dose	17.7 ± 1.2	17.5 ± 1.2	17.8 ± 1.2	0.463
Peripheral isodose line (%)	49.9 ± 3.3	50 ± 3.3	49.9 ± 3.3	0.83
Max dose	35.4 ± 2.8	35.5 ± 2.8	35.6 ± 2.9	0.434
Mean dose	22.6 ± 1.1	23.0 ± 0.9	22.4 ± 1.2	0.035
12 Gy volume	37.9 ± 21.3	31.0 ± 9	43.3 ± 26.2	0.06
% of nidus in 16 Gy line	97.6 ± 3.4	98.4 ± 2.1	97 ± 4	0.23
% of nidus in 18 Gy line	91.3 ± 2.6	93.0 ± 4.4	89.9 ± 7	0.94
% of nidus in 20 Gy line	81.3 ± 9.9	83.6 ± 7.1	79.5 ± 11.3	0.11
First stage volume	14.8 ± 4.6	14.0 ± 2.9	15.4 ± 5.6	0.64
2nd stage volume	15.4 ± 6.1	11.4 ± 2.7	17.0 ± 6.4	0.008
Interval between first and 2nd stage	4.8 ± 1.5	4.9 ± 1.7	4.7 ± 1.4	0.84

Data was presented as mean ± standard deviation

Table 3 Outcome of GKRS radiosurgery in two groups

	Total (n = 75)	Groups		P value
		Hemorrhage(n = 33)	Seizure(n = 42)	
Post GK symptom	11(14.7%)	6(18.2%)	5(11.9%)	0.52
MRI severe edema	16(21.3%)	11(33.3%)	5(11.9%)	0.025
MRI cyst formation	4(5.3%)	2(6.1%)	2(4.8%)	1
Post GK ICH	8(10.7%)	4(12.1%)	4(9.5%)	0.725
Expired	3(4%)	2(6.1%)	1(2.4%)	0.0579
Angiography outcome				0.94
Total obliteration	40(53.3%)	19(57.6%)	21(50%)	
Volume reduction	28(37.3%)	10(30.3%)	18(42.9%)	
No Change	7(9.3%)	4(12.1%)	3(7.1%)	

Data was presented as mean ± standard deviation

Imaging outcome

With MRA evidence of obliteration, 40 patients (53.3%) achieved angiography-confirmed obliteration (Fig. 2). Volume reduction was found in another 20 (Fig. 4), while 7 patients exhibited no volume change (Fig. 6). Sixteen patients (21.3%) developed severe brain edema at a median follow-up of 99 (72–150) months. Two of these cases required craniotomy for symptomatic relief (Fig. 7). Four patients (10.6%) developed cystic formations at median follow up of 103(80–150) months, with one patient undergoing a cyst-peritoneal shunt procedure (2.6%) (Fig. 3). New hemorrhages occurred in 8 patients (10.6%) (Fig. 4), with 4 of these (12.1%) in patients with a prior history of hemorrhage (annual bleeding rate of 1.2%) and 4 (9.5%) in patients with a history of seizures (annual bleeding rate of 1.1%). Kaplan-Meier analyses revealed that the hemorrhage incidence after GKRS

radiosurgery in the hemorrhage group approached that of the seizure group, indicating a beneficial effect in preventing re-hemorrhage in ruptured AVM (Fig. 8).

Imaging and clinical outcomes stratified by volume

Details of the imaging and clinical outcomes stratified by treatment algorithm are shown in Table 4. Of the 32 cases with nidus volumes between 10 and 15 cc, 25 (78.1%) achieved total obliteration. Five of the 8 cases of severe brain edema resulted in post GK symptoms. Among the 17 cases with volumes between 15 and 20 cc, 7 out of 15 cases treated with a single stage showed total obliteration, while none of the two-stage treatments (2 patients) resulted in complete obliteration. Three cases developed severe brain edema, while 2 cases with symptom in two stage groups. On case after two stages treatment showed permanent neurological deficits. Of the 26 cases with nidus volumes greater than 20 cc treated by two-stage procedures, only 8 (30.8%) achieved total obliteration. All 3 cases of severe brain edema in this group had led to post GKRS symptoms.

Risk factor analysis

In the univariate logistic regression analysis, total obliteration was significantly correlated with the following: smaller nidus volumes (less than 15 cc), single-stage treatment, the Radiosurgery-Based Grading Scale, first-stage volume, maximum dose, 12 Gy volume, and coverage percentages at 20 Gy, 18 Gy, and 16 Gy. However, multivariate analysis showed no significant differences (Table 5).

Cox regression analysis revealed that post GKRS symptoms were significantly correlated with the following: Virginia Radiosurgery AVM Score, Charlson Comorbidity Index, and mean radiation dose in both univariate and multivariate analyses (Table 6). Severe brain edema, detected via MRI, was also correlated with these same factors (Table 7).

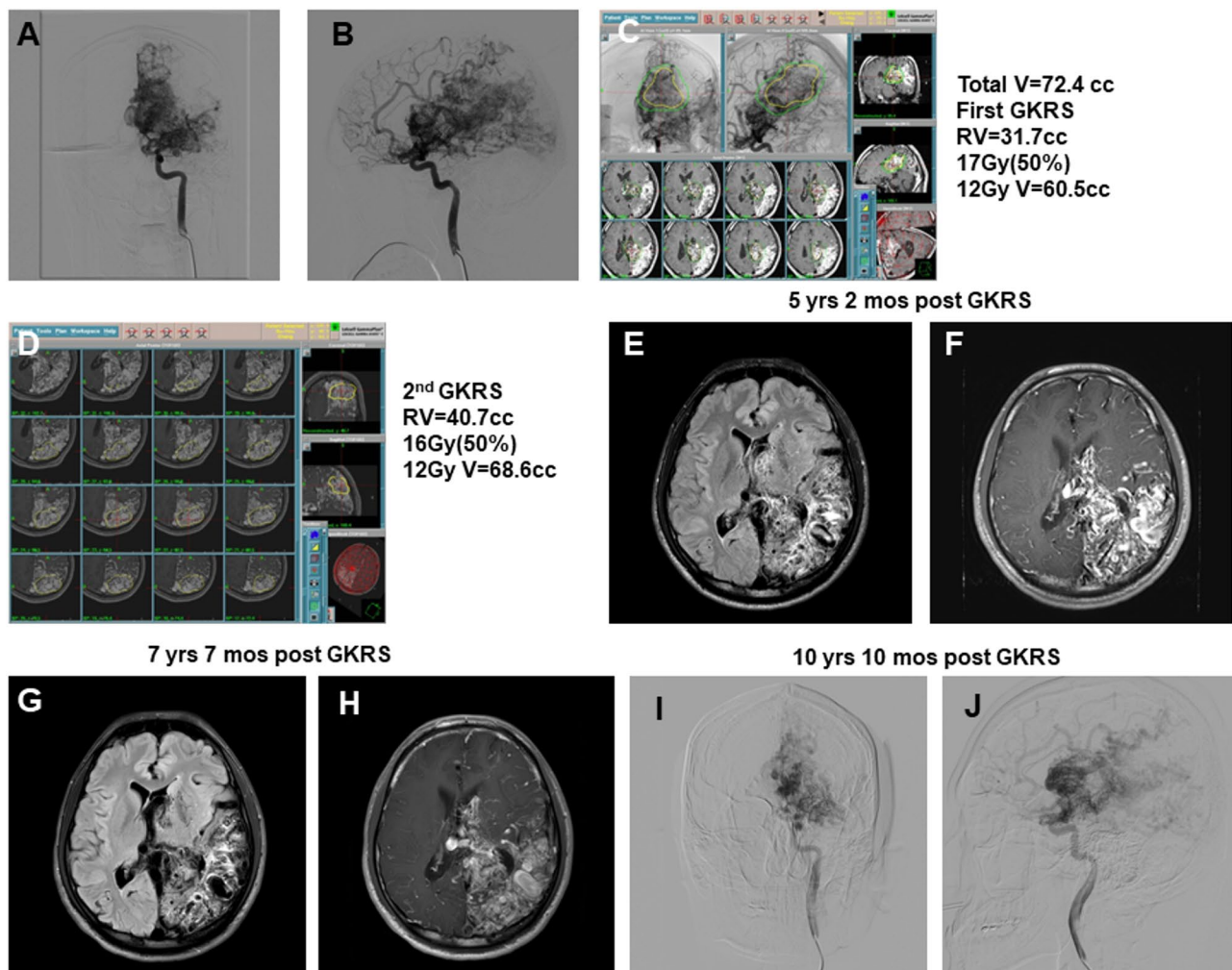


Fig. 6 A 24-year-old female with the generalized tonic seizure and diagnosed as a huge AVM with volume of 72.4 cc under the guidance of AVM volume > 20 cc treated in two stage gamma knife treatment. The post GKRS imaging showed the no definite obliteration with Engle II in seizure control. **(A)** A large AVM located in the left parietal-occipital region was observed in the anteroposterior view of cerebral angiography. It was supplied by feeders from the left anterior, middle, and posterior cerebral arteries, with venous drainage into the internal cerebral veins and the superior sagittal sinus. **(B)** A large AVM in the left parietal-occipital region was visualized in the lateral view of cerebral angiography, with arterial supply from the left anterior, middle, and posterior cerebral arteries, and venous drainage into the internal cerebral veins and the superior sagittal sinus. **(C)** Photograph showing dose planning for the first stage of Gamma Knife radiosurgery. Treatment parameters are displayed on the right side of the image. The yellow line indicates the 50% isodose line. **(D)** Photograph showing dose planning for the second stage of Gamma Knife radiosurgery. Treatment parameters are illustrated on the right side of the image. The yellow line represents the 50% isodose line. **(E)** No definite abnormal signal surrounding the nidus was detected on FLAIR MRI 5 years and 2 months after GKRS. **(F)** Persistent vascular structure-like enhancement in the left parietal region was observed on contrast-enhanced T1-weighted MRI 5 years and 2 months after GKRS. **(G)** No definite abnormal signal surrounding the nidus was seen on FLAIR MRI 7 years and 3 months after GKRS. **(H)** Persistent vascular structure-like enhancement in the left parietal region was detected on contrast-enhanced T1-weighted MRI 7 years and 3 months after GKRS. **(I)** A persistent large AVM was identified in the anteroposterior view of cerebral angiography 10 years and 5 months after GKRS. **(J)** A persistent large AVM was again visualized in the anteroposterior view of cerebral angiography 10 years and 5 months after GKRS.

MRI-detected cystic formations were highly correlated with lower margin isodose line percentages ($45 \pm 4.1\%$ vs. $50.2 \pm 3\%$, $p=0.003$). Seizure-free outcomes were significantly associated with younger patient age, with a median age of 33 (range: 19–39) compared to 42 (range: 24–50) ($p=0.023$). A lower Charlson Comorbidity Index was associated with reduced mortality (0.5 ± 1.1 vs. 2 ± 2.0 , $p=0.04$). An increased incidence of recurrent intracerebral hemorrhage was correlated with higher Virginia

Radiosurgery AVM Scores (3.5 ± 0.8 vs. 3 ± 0.6 , $p=0.047$), a higher Charlson Comorbidity Index (2 ± 2.4 vs. 0.4 ± 0.8 , $p=0.007$), and lower nidus coverage percentages at 16 Gy ($94.6 \pm 4.8\%$ vs. $97.9 \pm 3.0\%$, $p=0.006$) and 18 Gy ($87 \pm 6.6\%$ vs. $91.8 \pm 6.0\%$, $p=0.043$).

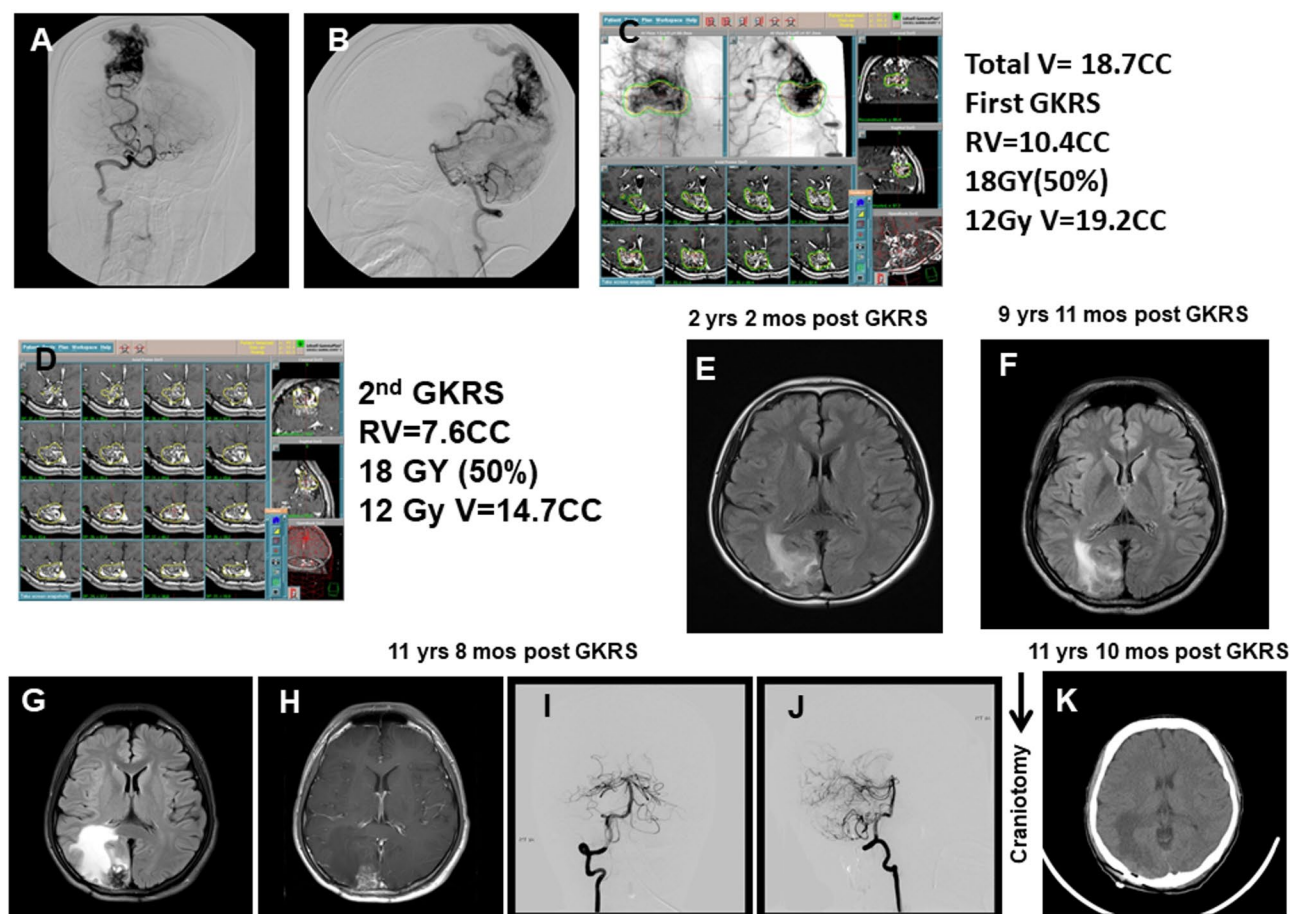


Fig. 7 A 12-year-old female presented with generalized seizure and diagnosed as huge AVM with volume of 15.8 cc. The treatment was separated into 2 stages under the guidance of AVM volume 15–20 cc in eloquent locations treated in two stages treatment. The imaging showed the total obliteration but severe brain edema mandatory of craniotomy to lessen the symptom. **(A)** A large AVM was detected in the right occipital region on the anteroposterior view of cerebral angiography, with arterial supply from the posterior cerebral artery and venous drainage into the superior sagittal sinus. **(B)** A large AVM was observed in the right occipital region on the lateral view of cerebral angiography, with feeders from the posterior cerebral artery and drainage into the superior sagittal sinus. **(C)** Photograph showing dose planning for the first stage of Gamma Knife radiosurgery. Treatment parameters are illustrated on the right side of the image. The yellow line indicates the 50% isodose line. **(D)** Photograph showing dose planning for the second stage of Gamma Knife radiosurgery. Treatment parameters are illustrated on the right side of the image. The yellow line indicates the 50% isodose line **(E)** An abnormal signal surrounding the nidus was detected in the right occipital region on FLAIR MRI one year and 6 months after GKRS. **(F)** A persistent abnormal signal, without increase in size, surrounding the nidus was seen on FLAIR MRI 9 years and 5 months after GKRS. **(G)** An increase in the abnormal signal surrounding the nidus was noted on FLAIR MRI 10 years and 10 months after GKRS. **(H)** A vascular structure-like enhancement in the right occipital region was detected on contrast-enhanced T1-weighted MRI 10 years and 10 months after GKRS. **(I)** No definite nidus was observed in the anteroposterior view of cerebral angiography 10 years and 10 months after GKRS. **(J)** No definite nidus was seen in the lateral view of cerebral angiography 10 years and 10 months after GKRS. The patient experienced intractable headache and underwent craniotomy for removal of the enhancing lesion. **(K)** No evidence of intracerebral hemorrhage (ICH) was found on brain CT one day after the operation. The patient experienced significant improvement in headache symptoms

Discussion

This study evaluated the outcomes of 75 patients with large symptomatic arteriovenous malformations (AVMs) treated using Gamma Knife radiosurgery (GKRS) as the first line treatment following the Taiwan Neurosurgical Consensus guidelines. The key results showed that total obliteration rates varied significantly according to AVM volume: 78.1% for volumes between 10 and 15 cc, 41.2% for 15 to 20 cc, and 30.8% for volumes greater than 20 cc. Severe brain edema developed in 21.3% of patients, with 14.6% experiencing post GK symptoms. Seizure free

control was achieved in 50% of patients, and the overall annual bleeding rate was low (1.2% for those with a history of hemorrhage and 1.1% for those with a history of seizures). Statistical analyses identified key factors for the total obliteration as follow up: smaller nidus volume, single-stage treatment, and coverage percentages at high radiation doses, while Virginia Radiosurgery AVM Score, Charlson Comorbidity Index, and mean radiation dose were significantly associated with complications such as brain edema and post GK symptoms.

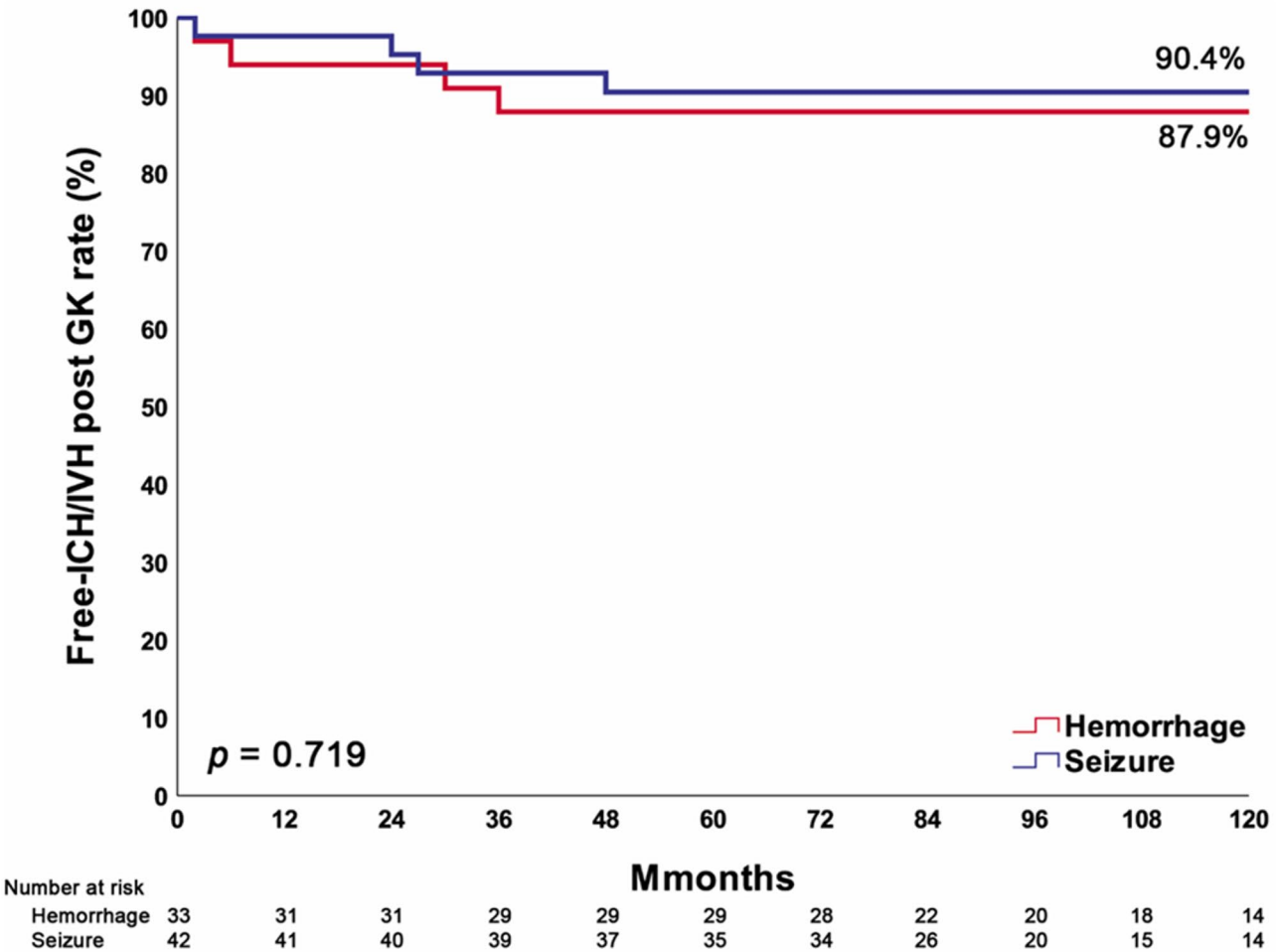


Fig. 8 Plot of incidence of hemorrhage related to time in huge AVM treated with GKRS. Y axis: rate of free hemorrhage (ICH/IVH) after GK
X: Time presented in months

Table 4 Imaging and clinical outcome stratified by volume

	10-15 cc (n=32)		15-20 cc (n=17)		> 20 cc (n=26)		p value
	n	%	n	%	n	%	
Angiography total obliteration	25	78.1%	7	41.2%	8	30.8%	0.001
MRI severe edema	8	25.0%	3	20.0%	3	11.5%	0.056
MRI Cyst	1	3.1%	2	11.8%	1	3.8%	0.435
Post GK hemorrhage	3	9.4%	2	11.8%	3	11.5%	1.0
Post GK symptom	5	15.6%	2	13.3%	3	11.5%	0.447

Chi-Square test. Fisher exact test. * $p < 0.05$, ** $p < 0.01$

Annual hemorrhage rates in AVMs range from less than 1% in unruptured, superficial AVMs to 33% in ruptured, deep-seated AVMs with venous drainage [2, 3]. Deep AVMs, like those in the basal ganglia, thalamus, or brainstem, carry a higher risk of hemorrhage, which can lead to neurological deficits in 50% of cases and a 10% fatality rate [4, 5]. Younger patients with deep AVMs or silent intralesional hemorrhages are at higher risk of future hemorrhage [3, 30]. For Spetzler-Martin Grade IV and V AVMs, hemorrhage risks range from 1.5% to 10.4% for non-hemorrhagic cases and 6–13.9% for prior

hemorrhages, making intervention critical [11, 31]. Small AVMs (≤ 3 cm) can be effectively treated with stereotactic radiosurgery (SRS) [32]. Post-SRS hemorrhage rates vary, but latent period rates range from 2.6 to 10% [33, 34]. A pooled analysis reported an annual hemorrhage rate of 1.4% post-GKRS [8], with a 2.5% risk until AVM obliteration [35]. Another study reported a reduction in hemorrhage rates from 3.4 to 1.3% after GKRS [20]. In our study on large AVMs, the annual hemorrhage rates were 1.2% for ruptured and 1.1% for unruptured AVMs, supporting the use of GKRS for large AVMs.

Table 5 Risk factors for angiography total obliteration

	Simple model			Multiple model		
	OR	(95% CI)	<i>p</i> value	OR	(95% CI)	<i>p</i> value
Group						
Hemorrhage	1.00					
Seizure	0.74	(0.29- 1.84)	0.514			
Size						
10-15 cc	1.00					
15-20 cc	0.20	(0.05- 0.70)	0.013			
> 20 cc	0.12	(0.04- 0.41)	0.001			
Stage						
Single	1.00					
Two stages	0.22	(0.08- 0.59)	0.003			
Location scores						
frontal/temporal	1.00					
parietal/occipital/corpus callosum/cerebellar	0.33	(0.12- 0.95)	0.039			
basal ganglia/thalamus/brainstem	0.94	(0.19- 4.76)	0.942			
Spetzler Martin grading	0.51	(0.23- 1.14)	0.099			
Radiosurgery-Based Grading Scale	0.35	(0.18- 0.68)	0.002	0.87	(0.19- 4.03)	0.862
Virginia Radiosurgery AVM Score	0.66	(0.32- 1.35)	0.257			
Neurological deficits before GK	2.07	(0.68- 6.28)	0.198			
Previous operation	2.36	(0.43- 13.00)	0.325			
Charlson comorbidity index	0.99	(0.67- 1.44)	0.938			
Number of feeding artery	0.65	(0.37- 1.17)	0.152			
Number of drainage veins	0.75	(0.29- 1.95)	0.562			
Number of Deep vein drainage	0.81	(0.35- 1.85)	0.614			
First stage volume (cc)	0.83	(0.72- 0.96)	0.011*	0.97	(0.80- 1.17)	0.739
Peripheral dose (Gy)	1.51	(1.00- 2.28)	0.050			
Peripheral dose line (%)	0.90	(0.77- 1.05)	0.173			
Maximum dosage (Gy)	1.27	(1.06- 1.54)	0.011	1.13	(0.92- 1.40)	0.245
Mean dosage (Gy)	1.16	(0.76- 1.76)	0.484			
12 Gy volume (cc)	0.95	(0.91- 0.99)	0.008			
16 Gy (%)	1.32	(1.08- 1.60)	0.006			
18 Gy (%)	1.12	(1.03- 1.21)	0.011			
20 Gy (%)	1.08	(1.02- 1.14)	0.007			

Logistic regression. * $p < 0.05$, ** $p < 0.01$

Patients with large, asymptomatic AVMs are often managed conservatively, as risks of interventions—such as embolization, surgery, or radiosurgery—can be equal to or exceed the natural risk of hemorrhage [36, 37]. While some studies suggested smaller AVMs have higher feeding artery pressure and hemorrhage risk [38], others reported no size correlation or even higher risk for larger AVMs [39, 40]. The dilemma is particularly challenging for unruptured hemispheric AVMs, which have a low annual hemorrhage rate of less than 1%. The lifetime rupture risk for a 35-year-old with a large, unruptured AVM was estimated at 35% [41] and, corroborated by a study showing a 24% rupture rate over 20 years [11]. After radiosurgery, hemorrhage risks increase temporarily, with rates of 4.6% and 5.3% in the first and second years [42]. A meta-analysis reported a 5.8% hemorrhage rate post-stereotactic radiosurgery (SRS), higher than after microsurgery (0%) and embolization (1.9%) [43].

Hemorrhage risk during the latent period increases with age and AVM size but decreases with higher radiation doses [44]. Prior AVM rupture was not a predictor of post-radiosurgery hemorrhage [45]. In our study, the annual bleeding rate after GKRS was 1.2% (unruptured AVM, seizure group), which is lower than those reported in the literature, suggesting that radiosurgery not only does not increase but may actually help prevent future hemorrhages in large, unruptured AVMs.

In SRS, treatment outcomes are closely tied to the relationship between the prescription dose and the target volume. This relationship becomes more challenging for larger arteriovenous malformations (AVMs) (greater than 3.5 cm in diameter or volume > 10 cc), often leading to lower cure rates and higher complication rates [32, 46–52]. However, the effectiveness of SRS drops with increasing AVM sizes. For deep-seated AVMs with volumes between 4 and 8 cm³, 25% of patients experienced

Table 6 Risk factors for post GKRS symptom

	Simple model			<i>p</i> value	Multiple model			<i>p</i> value
	HR	(95% CI)			HR	(95% CI)		
Seizure vs. Hemorrhage	0.67	(0.20-	2.19)	0.503				
Size								
10-15 cc	1.00							
15-20 cc	1.06	(0.25-	4.44)	0.939				
> 20 cc	0.67	(0.16-	2.81)	0.583				
Two stage vs. Single	0.83	(0.24-	2.84)	0.769				
Spetzler Martin grading	2.18	(0.92-	5.18)	0.076				
Radiosurgery-Based Grading Scale	0.90	(0.51-	1.58)	0.708				
Virginia Radiosurgery AVM Score	4.04	(1.39-	11.73)	0.010*	5.40	(1.81-	16.12)	0.002
Age (years)	1.02	(0.98-	1.06)	0.302				
Female vs. Male	1.16	(0.35-	3.79)	0.810				
Charlson comorbidity index	1.78	(1.28-	2.48)	0.001	2.45	(1.57-	3.83)	< 0.001
Number of feeding artery	0.70	(0.30-	1.67)	0.425				
Number of drainage veins	2.49	(0.93-	6.69)	0.070				
Number of Deep vein drainage	2.17	(0.79-	5.95)	0.133				
First stage volume (cc)	0.97	(0.83-	1.12)	0.653				
Peripheral dose (Gy)	1.06	(0.65-	1.73)	0.824				
Peripheral dose line (%)	1.07	(0.90-	1.27)	0.452				
Maximum dosage (Gy)	0.96	(0.78-	1.19)	0.726				
Mean dosage (Gy)	2.17	(1.25-	3.76)	0.006	2.58	(1.39-	4.77)	0.003
12 Gy volume (cc)	0.99	(0.95-	1.03)	0.491				
16 Gy (%)	0.90	(0.79-	1.03)	0.127				
18 Gy (%)	0.96	(0.88-	1.04)	0.337				
20 Gy (%)	0.98	(0.93-	1.04)	0.505				

Cox regression. **p* < 0.05, ***p* < 0.01

persistent adverse radiation effects (AREs), with the rate increasing to 33% for AVMs larger than 8 cm³ [53]. For AVMs exceeding 10 cm³, treatment outcomes are more inferior, characterized by a lower obliteration rate and higher morbidity [19, 54-56]. Consequently, single session radiosurgery is generally not recommended for AVMs larger than 10 cm³ [18]. Nonetheless, improved outcomes have been reported for AVMs smaller than 20 cm³. In these cases, a 76% obliteration rate was achieved within five years, with only 2% of patients experiencing persistent AREs [57]. For AVMs larger than 15 cm³, obliteration was achieved in only 25% of cases, with 37% of patients experiencing moderate and 12% experiencing severe adverse radiation effects [58]. Tailored strategies are necessary when treating AVMs with volumes between 10 and 20 cm³. In our treatment algorithm, AVMs with volumes under 20 cm³ were selected for single-session radiosurgery. However, for AVMs located in eloquent brain regions, a volume staged treatment approach was employed to minimize the risk of adverse effects and maximize treatment safety.

Obliteration rates of large AVMs treated with VS-SRS are similar to those achieved with the historical procedure of SS-SRS. However, VS-SRS offers a lower rate of AREs [53]. VS-SRS has been developed to enhance the efficacy and safety of treating large AVMs [20, 53, 59-65].

In accumulated data on VS-SRS for large AVMs, complete obliteration rates ranged from 28 to 62.5% [16, 20, 53, 61, 62, 65, 66]. In our study, guided by the Taiwan Neurosurgical Consensus, lesions larger than 20 cm³ were treated with staged Gamma Knife radiosurgery, showing an obliteration rate of 30.8%, which is lower than those reported in the literature. Such a discrepancy in results may be due to variations in volume criteria for staged stereotactic radiosurgery, highlighting the need for detailed categorization of AVM sizes to further investigate the relationship between obliteration rate and AVM size.

Several studies have reported potential challenges in VS-SRS for arteriovenous malformations (AVMs) [19, 20, 60]. One unresolved issue is the effect of blood redistribution from the untreated nidus on the success of VS-SRS. Hemorrhage risk was found to be higher in partially treated AVMs (26%) compared to those that were fully irradiated (5%) [46]. However, Pollock and Kano separately reported significantly lower hemorrhage rates in the untreated components of AVMs, with only one patient in each of the two studies experiencing post-treatment hemorrhage [19, 20]. A major limitation of VS-SRS is the prolonged latency period before AVM obliteration, during which hemorrhage poses a substantial risk [62]. Recent innovations, such as targeted

Table 7 Severe brain edema detected by MRI

	Simple model			<i>p</i> value	Multiple model			<i>p</i> value
	HR	(95% CI)			HR	(95% CI)		
Seizure vs. Hemorrhage	0.40	(0.14-	1.15)	0.089				
Size								
10-15 cc	1.00							
15-20 cc	1.06	(0.35-	3.26)	0.916				
> 20 cc	0.41	(0.11-	1.54)	0.185				
Location scores								
frontal/temporal	1.00							
parietal/occipital/corpus callosum/cerebellar	3.27	(0.89-	11.98)	0.074				
basal ganglia/thalamus/brainstem	3.19	(0.51-	19.94)	0.215				
Two vs. Single stage	0.86	(0.31-	2.36)	0.762				
Spetzler Martin grading	1.71	(0.81-	3.60)	0.157				
Radiosurgery-Based Grading Scale	0.79	(0.45-	1.37)	0.393				
Virginia Radiosurgery AVM Score	3.04	(1.28-	7.20)	0.011*	3.27	(1.36-	7.87)	0.008
Age (years)	1.01	(0.98-	1.04)	0.420				
Female vs. Male	0.82	(0.30-	2.27)	0.708				
History of ICH	1.52	(0.56-	4.09)	0.410				
Previous operation	1.34	(0.30-	5.93)	0.697				
Charlson comorbidity index	1.43	(1.02-	1.99)	0.037	1.62	(1.11-	2.37)	0.013
Number of feeding artery	1.21	(0.69-	2.12)	0.498				
Number of drainage veins	1.06	(0.39-	2.87)	0.912				
Number of Deep drainage veins	1.34	(0.56-	3.22)	0.514				
First stage volume (cc)	0.96	(0.84-	1.09)	0.490				
Peripheral dose (Gy)	0.97	(0.64-	1.46)	0.872				
Peripheral dose line (%)	0.99	(0.85-	1.14)	0.854				
Maximum dosage (Gy)	1.01	(0.85-	1.21)	0.911				
Mean dosage (Gy)	1.82	(1.16-	2.86)	0.009	1.74	(1.10-	2.77)	0.018
12 Gy volume (cc)	0.99	(0.95-	1.02)	0.394				
16 Gy (%)	1.07	(0.90-	1.27)	0.458				
18 Gy (%)	1.02	(0.94-	1.11)	0.643				
20 Gy (%)	1.00	(0.96-	1.05)	0.905				

Cox regression. * $p < 0.05$, ** $p < 0.01$

embolization of intranidal aneurysms or more aggressive treatment of AVM fistulas and proximal aneurysms, may help reduce this risk [20, 62]. Additionally, strategies like shortening the interval between treatment stages and compartmentalizing AVMs into smaller target volumes with lower radiation doses have been shown to be safer and more effective [60, 62]. In our study, most hemorrhages occurred within 36 months, independent of single-stage or two-stage treatments. However, there was no significant difference in hemorrhage risk between the hemorrhage and seizure groups, suggesting that VS-SRS does not increase hemorrhage risk during the latent period. Nevertheless, the optimal timing for the second treatment stage remains uncertain and requires further investigation.

Dose-volume guidelines for cerebral AVMs have been previously reported [48, 67, 68]. The most critical factor associated with obliteration after stereotactic radiosurgery (SRS) is the radiation dose delivered to the AVM. Typically, a radiation dose of 22 Gy (at the 50% isodose

line) is used in single-session treatments for cerebral AVMs. However, increasing the dose to 25 Gy does not improve obliteration rates and is associated with a higher risk of complications [67]. The “12 Gy volume” is recognized as the most important factor in symptomatic radiation injury. Efforts have been made to minimize the amount of normal brain tissue receiving more than 12 Gy. Staged treatments help reduce the volume receiving 12 Gy, regardless of the number of stages [55], with the advantage of keeping the composite 12 Gy volume under 10% of the brain volume in all patients. This parameter continues to be a key factor to consider in treatment planning and evaluation, especially as experience grows with staged treatments for large AVMs [34]. In our study, to balance increased obliteration with minimizing radiation effects, we used staged doses ranging from 16 to 20 Gy, tailored to the nidus volume, to approach the dosage required for AVM obliteration.

Complete AVM obliteration was defined using MRI-weighted images, specifically the disappearance of flow

voids on T2-weighted images. In contrast, complete angiographic AVM obliteration was defined as the disappearance of the nidus and the absence of early venous drainage [20, 42, 69]. Conventional angiography remains the gold standard for confirming complete AVM obliteration [20]. However, not all patients undergo angiography, particularly those in poor overall health, and some may even decline follow-up angiography. Fortunately, MRI has shown a predictive value for obliteration as high as 97%, with repeat angiography often revealing key features of obliteration, such as the absence of early venous drainage [19]. In our study, angiography was used as the definitive diagnostic procedure to confirm complete obliteration. This might have influenced the obliteration rate, particularly in cases where drainage veins were involved, as angiography ultimately provided the final confirmation.

Favorable seizure outcomes following radiosurgery have been reported in previous studies, with success rates reaching up to 80% [70–72]. These outcomes have been closely correlated with AVM obliteration. Similar results have been observed in patients with large AVMs [16]. Seizure control was achieved in 67% of patients [65]. Clinical improvement has been reported in nearly half of the patients, likely due to the occlusive effect of radiosurgery on the AVM, which alters its hemodynamics and reduces the “steal” effect on cerebral circulation [73]. This phenomenon has been documented in other studies, though with slightly higher rates of improvement [16]. Factors that increase the risk of seizures in patients with AVMs include male gender, younger age, frontal or temporal lobe AVMs, AVMs located in the brain cortex, superficial venous drainage, a superficial temporal lobe AVM nidus, fistulous AVMs, and AVMs with venous stenosis [9, 10, 14, 74–76]. Some studies also identify larger AVMs (> 3 cm) as an independent predictor of seizures [13, 14]. In our study, only 50% of patients reach the stage of complete seizure-free. However, when including the 47.6% of patients classified as Engel II in the seizure assessment, the overall favorable seizure outcome reached 97.6%, aligning closely with reports in the literature. However, since GKRS was performed just 2–3 weeks after the seizure episode, the interval before GKRS treatment was too short to provide sufficient information for determining the Engel classification before and after treatment. In our series, young age was the only factor associated with a favorable seizure-free outcome. This may be a confounding factor, as the incidence of seizures is higher in younger subjects.

Post-radiosurgery complications include brain edema, radiation necrosis, arterial stenosis, delayed cyst formation, radiation induced neoplasia, and organizing hematoma [48, 77, 78]. Two mechanisms have been suggested: direct radiation injury to adjacent brain tissue and hemodynamic changes following irradiation [79]. Radiation

damage to oligodendrocytes and subsequent glial cell reactions may cause edema, necrosis, and cyst formation, while damage to endothelial cells can lead to arterial stenosis, encapsulated hematomas, and hemorrhage after AVM obliteration [77, 80, 81]. The incidence of radiological complications ranges from 30 to 40%, while symptomatic complications are reported at 8.1 to 11.8% [45, 77, 80]. Long-term complications of SRS include 3.4% delayed cyst formation, 1.7% higher seizure activity, and 0.4% signal change in white matter [48, 82]. New nidus development around the obliterated area has also been reported [83]. In our study, cyst formation and persistent white matter signal changes were the most common long-term complications. Only one of 4 cysts and 2 of 21 patients with T2 changes required surgery. These results underscore the importance of long-term follow-up for large AVMs treated with GKRS.

In Gamma Knife radiosurgery (GKRS) for arteriovenous malformations (AVMs), the peripheral radiation dose and mean radiation dose are directly influenced by the number of shots and the collimator size used in treatment planning [67, 84]. The interplay of these factors determines dose distribution, treatment efficacy, and complication risks. To achieve better conformity in treating large AVMs, a higher number of shots and the use of smaller collimators are necessary [85]. This approach enhances dose precision but also results in an elevated mean radiation dose. In our Cox regression analysis, post-GKRS edema and symptomatic episodes were highly correlated with the mean radiation dose, aligning with the goal of achieving better conformity, particularly in the treatment of large AVMs.

Grading scales integrate individual predictors of outcome into an overall grade or score, which correlates with posttreatment outcomes and, ultimately, serves to guide

management decisions [21, 23, 86]. The first, and most widely used, AVM grading system was described by Spetzler and Martin [23]. Although this grade has been shown to correlate with AVM GKRS outcomes, it was originally proposed as a grading system for predicting operative morbidity and mortality after surgical intervention [20, 23]. Thus, the grades may not entirely reflect factors that most significantly affect outcomes after AVM GKRS. Subsequently, the Radiosurgery-Based Grading Scale (RBAS) was developed specifically for AVMs treated with radiosurgery and grades correlate with outcomes after GKRS, with accuracy comparable to that of the Spetzler-Martin grading system [19, 21, 87]. RBAS is calculated using a formula that incorporates patient age, AVM volume, and location eloquence. This continuous scoring system provides a nuanced assessment of the AVM's complexity. Research indicates that the RBAS effectively predicts AVM obliteration without new neurological deficits post-radiosurgery. For example, patients

with an RBAS of 1.0 or less had a 62% rate of obliteration without new deficits, whereas those with scores greater than 2.0 had a 32% rate [19]. VRAS was designed to be a practical grading system analogous to the Spetzler-Martin grading scale. VRAS, unlike RBAS being a tool for assessing the suitability of an AVM nidus for treatment with GKRS, is affected more by a number of factors, like AVM nidus volume, eloquent location, and prior AVM hemorrhage than AVM maximum diameter, deep venous drainage, deep AVM location, and patient age. The VRAS assigns points based on specific AVM characteristics: 1 point each for an AVM volume of 2–4 cm³, eloquent AVM location, or a history of hemorrhage, and 2 points for an AVM volume greater than 4 cm³. For instance, 80% of patients with a score of 0–1 achieved favorable results, compared to 45% with scores of 3–4 [25]. In summary, the VRAS is particularly useful for predicting post-radiosurgery complications, aiding in risk assessment and patient counseling. Conversely, the RBAS excels in predicting the likelihood of complete AVM obliteration, assisting clinicians in treatment planning and prognostication. Using both grading scales in a complementary manner provides a more comprehensive evaluation of potential outcomes for patients undergoing radiosurgical treatment for AVMs. In our study, VRAS appeared to be a superior predictor of post-radiosurgery edema and its associated symptoms in large AVMs treated with Gamma Knife. This finding aligns with its strong predictive power in assessing post-radiosurgical complications.

The Charlson Comorbidity Index (CCI) is a widely used tool for predicting mortality by classifying and weighting comorbid conditions. It assigns weighted scores (ranging from 1 to 6) to 17 different comorbidities based on their impact on a patient's one-year mortality risk, with the total score calculated by summing these weights [26]. While specific studies directly correlating CCI scores with outcomes of arteriovenous malformations (AVMs) treated by radiosurgery are limited, research indicates that patient frailty and comorbidities play a crucial role in treatment decisions and outcomes. One study analyzing the impact of the COVID-19 pandemic on Gamma Knife radiosurgery (GKRS) decision-making found that patients with higher CCI scores were more likely to proceed with GKRS without hesitation, despite the pandemic [27]. This suggests that patients with significant comorbidities may prioritize timely treatment due to their increased health risks. Additionally, research on patient frailty—often encompassing comorbidities assessed by tools like the CCI—has demonstrated that increased frailty is associated with higher complication rates and extended hospital stays in AVM patients undergoing microsurgery. Although this study focused on microsurgical interventions, it underscores the importance of considering comorbidities when evaluating

treatment options for AVMs [88]. Furthermore, patients with higher CCI scores often have a poorer baseline health status, increasing their risk of spontaneous hemorrhage and leading to worse neurological outcomes following AVM rupture [89]. Although the CCI is not specifically designed for AVM patients, it remains a valuable tool for assessing overall health status and potential risks associated with treatment. Clinicians should integrate both the CCI and AVM-specific factors to optimize patient care and outcomes. In this study, a high CCI was associated with an increased risk of post-GKRS symptoms and edema, aligning with findings in AVM patients treated with other modalities.

Study Limitations

There were several limitations in this study. First, previous studies have reported that two-stage volume treatment for lesions > 10 mL or > 15 mL, as well as three-stage treatment for lesions > 20 mL, can be effective [63, 64, 90]. However, under our insurance reimbursement policy, which follows the consensus of the Taiwan Neurological Society, AVM treatment is only covered for a single session. The cost of a second or third treatment session is not reimbursed and must be absorbed by the hospital. Consequently, we modified our treatment strategy to balance clinical outcomes with financial constraints. Second, our initial hypothesis aimed to investigate the hemorrhage rate between ruptured and unruptured AVM groups. To do so, we assumed the unruptured group consisted primarily of patients presenting with seizures. However, the true control group should have been patients with unruptured AVMs regardless of symptomatology. This introduced a confounding factor, potentially affecting the conclusion that the treatment outcomes for unruptured AVMs were comparable to those of the rupture group. Third, this study was a retrospective review conducted on a small cohort ($n=75$) from a single institution. Due to the limited sample size, we were unable to identify significant predictors of cyst formation, mortality incidence, or seizure-free outcomes using the Cox proportional hazards model. Therefore, further prospective studies with larger patient cohorts are necessary to validate our findings.

Conclusion

The obliteration rate of large AVMs treated with Gamma Knife is closely linked to AVM sizes. AVMs smaller than 15 cc responded well to single-stage treatment. Larger AVMs (> 15 cc) exhibited a lower obliteration rate but still low rates of hemorrhage and neurological complications. VARS grading system helped predicting post-treatment edema and symptoms. Despite lower obliteration rates in large AVMs, low complication rates support the potential for further Gamma Knife treatments, especially

in patients with significant nidus reduction. Such intervention may improve neurological function with minimal post-surgical complications, supporting Taiwan's consensus on treating large AVMs with Gamma Knife radiosurgery.

Abbreviations

AVMs	Arteriovenous malformations
GKRS	Gamma Knife radiosurgery
ICH	Intracerebral hemorrhage
Gy	Gray
MRI	Magnetic Resonance Imaging
TOF	Time-of-flight
SRS	Stereotactic radiosurgery
SVR	Staged volume radiosurgery
RBAS	Radiosurgery-Based Grading Scale
VRAS	Virginia Radiosurgery AVM Scale

Acknowledgements

The author would like to thank the Biostatistics Task Force of Taichung Veterans General Hospital for their kind assistance in statistical analysis.

Author contributions

Author Contributions MHS, YST and TWW prepared Figs. 1, 2 and 3. SYL, YJC, and CCS prepared Figs. 4 and 5. MYY prepared Tables 1, 2 and 3. WCY and MLS prepared Figs. 6, 7 and 8. JS prepared Table 4, and 5. HCP prepared Table 6, and 7. MHS and WCY wrote the main manuscript text. All authors reviewed the manuscript.

Funding

This work was supported by the grant MOST 111-2314-B-075 A-011-MY2 from the National Science and Technology Council, Taiwan and the grants TCVGH-1137307 C, TCVGH-NCHU1137603, TCVGH-PU1138101, TCVGH-1137303D, and TCVGH-113G412 from Taichung Veteran General Hospital, Taiwan.

Data availability

No datasets were generated or analysed during the current study.

Declarations

Ethics approval and consent to participate

This study was approved by the Ethical Committee of Taichung Veterans General Hospital (No. CE24566B).

Consent for publication

Not applicable.

Competing interests

The authors declare no competing interests.

Author details

¹Department of Neurosurgery, Neurological Institute, Taichung Veterans General Hospital, Taichung, Taiwan

²School of Medicine, College of Medicine, National Yang Ming Chiao Tung University, Taipei, Taiwan

³PhD program in Health and Social Welfare for Indigenous Peoples, Providence University, Taichung, Taiwan

⁴Department of Neurosurgery, University of Virginia, Charlottesville, VA, USA

⁵Department of Radiation Oncology, Taichung Veterans General Hospital, Taichung, Taiwan

⁶Institute of Biomedical Science, National Chung-Hsing University, Taichung, Taiwan

⁷Department of Medical Research, Taichung Veterans General Hospital, 1650 Taiwan Boulevard Sec.4, Taichung 40705, Taiwan

⁸Rong Hsing Research Center for Translational Medicine, National Chung-Hsing University, Taichung, Taiwan

Published online: 27 May 2025

References

1. Al-Shahi R, Bhattacharya JJ, Currie DG, Papanastassiou V, Ritchie V, Roberts RC, et al. Prospective, population-based detection of intracranial vascular malformations in adults: the Scottish intracranial vascular malformation study (SIVMS). *Stroke*. 2003;34:1163–9.
2. Ding C, Hryckushko B, Whitworth L, Li X, Nedzi L, Weprin B, et al. Multistage stereotactic radiosurgery for large cerebral arteriovenous malformations using the gamma knife platform. *Med Phys*. 2017;44:5010–9.
3. Stapf C, Mast H, Sciacca RR, Choi JH, Khaw AV, Connolly ES, et al. Predictors of hemorrhage in patients with untreated brain arteriovenous malformation. *Neurology*. 2006;66:1350–5.
4. Fukuda K, Majumdar M, Masoud H, Nguyen T, Honarmand A, Shaibani A, et al. Multicenter assessment of morbidity associated with cerebral arteriovenous malformation hemorrhages. *J Neurointerv Surg*. 2017;9:664–8.
5. Solomon RA, Connolly ES. Jr. Arteriovenous malformations of the brain. *N Engl J Med*. 2017;376:1859–66.
6. Mohr JP, Parides MK, Stapf C, Moquete E, Moy CS, Overbey JR, et al. Medical management with or without interventional therapy for unruptured brain arteriovenous malformations (ARUBA): a multicentre, non-blinded, randomised trial. *Lancet*. 2014;383:614–21.
7. Al-Shahi Salman R, White PM, Counsell CE, du Plessis J, van Beijnum J, Josephson CB, et al. Outcome after Conservative management or intervention for unruptured brain arteriovenous malformations. *JAMA*. 2014;311:1661–9.
8. Can A, Gross BA, Du R. The natural history of cerebral arteriovenous malformations. *Handb Clin Neurol*. 2017;143:15–24.
9. Galletti F, Costa C, Cupini LM, Eusebi P, Hamam M, Caputo N, et al. Brain arteriovenous malformations and seizures: an Italian study. *J Neurol Neurosurg Psychiatry*. 2014;85:284–8.
10. Garcin B, Houdart E, Porcher R, Manchon E, Saint-Maurice JP, Bresson D, et al. Epileptic seizures at initial presentation in patients with brain arteriovenous malformation. *Neurology*. 2012;78:626–31.
11. Laakso A, Dashti R, Juvela S, Isarakul P, Niemelä M, Hernesniemi J. Risk of hemorrhage in patients with untreated Spetzler-Martin grade IV and V arteriovenous malformations: a long-term follow-up study in 63 patients. *Neurosurgery*. 2011;68:372–7. discussion 378.
12. Sattari SA, Yang W, Xu R, Feghali J, Tamargo RJ, Huang J. Natural history and treatment of deep-seated brain arteriovenous malformations in pediatric patients. *J Neurosurg Pediatr*. 2022;30:578–85.
13. Fierstra J, Conklin J, Krings T, Slessarev M, Han JS, Fisher JA, et al. Impaired perinatal cerebrovascular reserve in seizure patients with brain arteriovenous malformations. *Brain*. 2011;134:100–9.
14. Hoh BL, Chapman PH, Loeffler JS, Carter BS, Ogilvy CS. Results of multimodality treatment for 141 patients with brain arteriovenous malformations and seizures: factors associated with seizure incidence and seizure outcomes. *Neurosurgery*. 2002;51:303–309; discussion 309–311.
15. Englot DJ, Young WL, Han SJ, McCulloch CE, Chang EF, Lawton MT. Seizure predictors and control after microsurgical resection of supratentorial arteriovenous malformations in 440 patients. *Neurosurgery*. 2012;71:572–80. discussion 580.
16. Franzin A, Panni P, Spatola G, Del Vecchio A, Gallotti AL, Gigliotti CR, et al. Results of volume-staged fractionated gamma knife radiosurgery for large complex arteriovenous malformations: obliteration rates and clinical outcomes of an evolving treatment paradigm. *J Neurosurg*. 2016;125:104–13.
17. Duffner F, Freudenstein D, Becker G, Ernemann U, Grote EH. Combined treatment effects after embolization and radiosurgery in high-grade arteriovenous malformations. Case report and review of the literature. *Stereotact Funct Neurosurg*. 2000;75:27–34.
18. Ogilvy CS, Stieg PE, Awad I, Brown RD Jr., Kondziolka D, Rosenwasser R, et al. AHA scientific statement: recommendations for the management of intracranial arteriovenous malformations: a statement for healthcare professionals from a special writing group of the stroke Council, American stroke association. *Stroke*. 2001;32:1458–71.
19. Pollock BE, Flickinger JC. A proposed radiosurgery-based grading system for arteriovenous malformations. *J Neurosurg*. 2002;96:79–85.
20. Kano H, Kondziolka D, Flickinger JC, Park KJ, Parry PV, Yang HC, et al. Stereotactic radiosurgery for arteriovenous malformations, part 6: multistaged volumetric management of large arteriovenous malformations. *J Neurosurg*. 2012;116:54–65.

21. Pollock BE, Flickinger JC. Modification of the radiosurgery-based arteriovenous malformation grading system. *Neurosurgery*. 2008;63:239–43. discussion 243.
22. Abila AA, Rutledge WC, Seymour ZA, Guo D, Kim H, Gupta N, et al. A treatment paradigm for high-grade brain arteriovenous malformations: volume-staged radiosurgical downgrading followed by microsurgical resection. *J Neurosurg*. 2015;122:419–32.
23. Spetzler RF, Martin NA. A proposed grading system for arteriovenous malformations. *J Neurosurg*. 1986;65:476–83.
24. Hartmann A, Stapf C, Hofmeister C, Mohr JP, Sciacca RR, Stein BM, et al. Determinants of neurological outcome after surgery for brain arteriovenous malformation. *Stroke*. 2000;31:2361–4.
25. Starke RM, Yen CP, Ding D, Sheehan JP. A practical grading scale for predicting outcome after radiosurgery for arteriovenous malformations: analysis of 1012 treated patients. *J Neurosurg*. 2013;119:981–7.
26. Charlson ME, Pompei P, Ales KL, MacKenzie CR. A new method of classifying prognostic comorbidity in longitudinal studies: development and validation. *J Chronic Dis*. 1987;40:373–83.
27. Shen CC, Jiang RS, Yang MY, You WC, Sun MH, Sheu ML, et al. Influence of COVID-19 pandemic on the decision making of patients in undergoing gamma knife radiosurgery. *Eur J Med Res*. 2022;27:223.
28. Buis DR, Bot JC, Barkhof F, Knol DL, Lagerwaard FJ, Slotman BJ, et al. The predictive value of 3D time-of-flight MR angiography in assessment of brain arteriovenous malformation obliteration after radiosurgery. *AJNR Am J Neuroradiol*. 2012;33:232–8.
29. Lim HK, Choi CG, Kim SM, Kim JL, Lee DH, Kim SJ, et al. Detection of residual brain arteriovenous malformations after radiosurgery: diagnostic accuracy of contrast-enhanced four-dimensional MR angiography at 3.0 T. *Br J Radiol*. 2012;85:1064–9.
30. Fleetwood IG, Marcellus ML, Levy RP, Marks MP, Steinberg GK. Deep arteriovenous malformations of the basal ganglia and thalamus: natural history. *J Neurosurg*. 2003;98:747–50.
31. Han PP, Ponce FA, Spetzler RF. Intention-to-treat analysis of Spetzler-Martin grades IV and V arteriovenous malformations: natural history and treatment paradigm. *J Neurosurg*. 2003;98:3–7.
32. Chang JH, Chang JW, Park YG, Chung SS. Factors related to complete occlusion of arteriovenous malformations after gamma knife radiosurgery. *J Neurosurg*. 2000;93(Suppl 3):96–101.
33. Bir SC, Ambekar S, Maiti TK, Nanda A. Clinical outcome and complications of gamma knife radiosurgery for intracranial arteriovenous malformations. *J Clin Neurosci*. 2015;22:1117–22.
34. Ding D, Starke RM, Kano H, Lee JY, Mathieu D, Pierce J, et al. Stereotactic radiosurgery for Spetzler-Martin grade III arteriovenous malformations: an international multicenter study. *J Neurosurg*. 2017;126:859–71.
35. Yen CP, Sheehan JP, Schwyzler L, Schlesinger D. Hemorrhage risk of cerebral arteriovenous malformations before and during the latency period after GAMMA knife radiosurgery. *Stroke*. 2011;42:1691–6.
36. de Oliveira E, Tedeschi H, Raso J. Comprehensive management of arteriovenous malformations. *Neurol Res*. 1998;20:673–83.
37. Hamilton MG, Spetzler RF. The prospective application of a grading system for arteriovenous malformations. *Neurosurgery*. 1994;34:2–6. discussion 6–7.
38. Spetzler RF, Hargraves RW, McCormick PW, Zabramski JM, Flom RA, Zimmerman RS. Relationship of perfusion pressure and size to risk of hemorrhage from arteriovenous malformations. *J Neurosurg*. 1992;76:918–23.
39. Jayaraman MV, Marcellus ML, Do HM, Chang SD, Rosenberg JK, Steinberg GK et al. Hemorrhage rate in patients with Spetzler-Martin grades IV and V arteriovenous malformations: is treatment justified? *Stroke* 2007; 38: 325–329.
40. Mast H, Young WL, Koennecke HC, Sciacca RR, Osipov A, Pile-Spellman J, et al. Risk of spontaneous haemorrhage after diagnosis of cerebral arteriovenous malformation. *Lancet*. 1997;350:1065–8.
41. Kondziolka D, McLaughlin MR, Kestle JR. Simple risk predictions for arteriovenous malformation hemorrhage. *Neurosurgery*. 1995;37:851–5.
42. Sirin S, Kondziolka D, Niranjan A, Flickinger JC, Maitz AH, Lunsford LD. Prospective staged volume radiosurgery for large arteriovenous malformations: indications and outcomes in otherwise untreatable patients. *Neurosurgery*. 2006;58:17–27. discussion 17–27.
43. van Beijnum J, van der Worp HB, Buis DR, Al-Shahi Salman R, Kappelle LJ, Rinkel GJ, et al. Treatment of brain arteriovenous malformations: a systematic review and meta-analysis. *JAMA*. 2011;306:2011–9.
44. Karlsson B, Lax I, Söderman M. Risk for hemorrhage during the 2-year latency period following gamma knife radiosurgery for arteriovenous malformations. *Int J Radiat Oncol Biol Phys*. 2001;49:1045–51.
45. Ding D, Yen CP, Starke RM, Xu Z, Sun X, Sheehan JP. Outcomes following single-session radiosurgery for high-grade intracranial arteriovenous malformations. *Br J Neurosurg*. 2014;28:666–74.
46. Colombo F, Pozza F, Chiarego G, Casentini L, De Luca G, Francescon P. Linear accelerator radiosurgery of cerebral arteriovenous malformations: an update. *Neurosurgery*. 1994;34:14–20. discussion 20–11.
47. Flickinger JC. An integrated logistic formula for prediction of complications from radiosurgery. *Int J Radiat Oncol Biol Phys*. 1989;17:879–85.
48. Izawa M, Hayashi M, Chernov M, Nakaya K, Ochiai T, Murata N, et al. Long-term complications after gamma knife surgery for arteriovenous malformations. *J Neurosurg*. 2005;102(Suppl):34–7.
49. Karlsson B, Lindquist C, Steiner L. Prediction of obliteration after gamma knife surgery for cerebral arteriovenous malformations. *Neurosurgery*. 1997;40:425–30. discussion 430–421.
50. Lunsford LD, Kondziolka D, Flickinger JC, Bissonette DJ, Jungreis CA, Maitz AH, et al. Stereotactic radiosurgery for arteriovenous malformations of the brain. *J Neurosurg*. 1991;75:512–24.
51. Marks LB, Spencer DP. The influence of volume on the tolerance of the brain to radiosurgery. *J Neurosurg*. 1991;75:177–80.
52. Steinberg GK, Fabrikant JL, Marks MP, Levy RP, Frankel KA, Phillips MH, et al. Stereotactic heavy-charged-particle Bragg-peak radiation for intracranial arteriovenous malformations. *N Engl J Med*. 1990;323:96–101.
53. Nagy G, Rowe JG, Radatz MW, Hodgson TJ, Coley SC, Kemeny AA. A historical analysis of single-stage γ knife radiosurgical treatment for large arteriovenous malformations: evolution and outcomes. *Acta Neurochir (Wien)*. 2012;154:383–94.
54. Han JH, Kim DG, Chung HT, Park CK, Paek SH, Kim JE, et al. Clinical and neuroimaging outcome of cerebral arteriovenous malformations after gamma knife surgery: analysis of the radiation injury rate depending on the arteriovenous malformation volume. *J Neurosurg*. 2008;109:191–8.
55. Jones J, Jang S, Getch CC, Kepka AG, Marymont MH. Advances in the radiosurgical treatment of large inoperable arteriovenous malformations. *Neurosurg Focus*. 2007;23:E7.
56. Kemeny AA, Radatz MW, Rowe JG, Walton L, Hampshire A. Gamma knife radiosurgery for cerebral arteriovenous malformations. *Acta Neurochir Suppl*. 2004;91:55–63.
57. Hanakita S, Koga T, Shin M, Igaki H, Saito N. Application of single-stage stereotactic radiosurgery for cerebral arteriovenous malformations > 10 cm³. *Stroke*. 2014;45:3543–8.
58. Pan DH, Guo WY, Chung WY, Shiau CY, Chang YC, Wang LW. Gamma knife radiosurgery as a single treatment modality for large cerebral arteriovenous malformations. *J Neurosurg*. 2000;93(Suppl 3):113–9.
59. Amponsah K, Ellis TL, Chan MD, Bourland JD, Glazier SS, McMullen KP, et al. Staged gamma knife radiosurgery for large cerebral arteriovenous malformations. *Stereotact Funct Neurosurg*. 2011;89:365–71.
60. Chung WY, Shiau CY, Wu HM, Liu KD, Guo WY, Wang LW, et al. Staged radiosurgery for extra-large cerebral arteriovenous malformations: method, implementation, and results. *J Neurosurg*. 2008;109(Suppl):65–72.
61. Hanakita S, Shin M, Koga T, Igaki H, Saito N. Outcomes of Volume-Staged radiosurgery for cerebral arteriovenous malformations larger than 20 cm³ with more than 3 years of Follow-Up. *World Neurosurg*. 2016;87:242–9.
62. Huang PP, Rush SC, Donahue B, Narayana A, Becske T, Nelson PK, et al. Long-term outcomes after staged-volume stereotactic radiosurgery for large arteriovenous malformations. *Neurosurgery*. 2012;71:632–43. discussion 643–634.
63. Moosa S, Chen CJ, Ding D, Lee CC, Chivukula S, Starke RM, et al. Volume-staged versus dose-staged radiosurgery outcomes for large intracranial arteriovenous malformations. *Neurosurg Focus*. 2014;37:E18.
64. Seymour ZA, Sneed PK, Gupta N, Lawton MT, Molinaro AM, Young W, et al. Volume-staged radiosurgery for large arteriovenous malformations: an evolving paradigm. *J Neurosurg*. 2016;124:163–74.
65. El-Shehaby AMN, Reda WA, Abdel Karim KM, Emad Eldin RM, Nabeel AM, Tawadros SR. Volume-Staged gamma knife radiosurgery for large brain arteriovenous malformation. *World Neurosurg*. 2019;132:e604–12.
66. Chytka T, Liscak R, Kozubiková P, Vymazal J. Radiosurgery for large arteriovenous malformations as a Single-Session or staged treatment. *Stereotact Funct Neurosurg*. 2015;93:342–7.
67. Flickinger JC, Kondziolka D, Maitz AH, Lunsford LD. An analysis of the dose-response for arteriovenous malformation radiosurgery and other factors affecting obliteration. *Radiother Oncol*. 2002;63:347–54.

68. Friedman WA, Bova FJ, Bollampally S, Bradshaw P. Analysis of factors predictive of success or complications in arteriovenous malformation radiosurgery. *Neurosurgery*. 2003;52:296–307. discussion 307–298.
69. Dalyai R, Theofanis T, Starke RM, Chalouhi N, Ghobrial G, Jabbour P et al. Stereotactic radiosurgery with neoadjuvant embolization of larger arteriovenous malformations: an institutional experience. *Biomed Res Int* 2014; 2014: 306518.
70. Baranoski JF, Grant RA, Hirsch LJ, Visintainer P, Gerrard JL, Günel M, et al. Seizure control for intracranial arteriovenous malformations is directly related to treatment modality: a meta-analysis. *J Neurointerv Surg*. 2014;6:684–90.
71. Ditty BJ, Omar NB, Foreman PM, Miller JH, Kicilinski KP, Fisher WS. Seizure outcomes after stereotactic radiosurgery for the treatment of cerebral arteriovenous malformations. *J Neurosurg*. 2017;126:845–51. 3rd et al.
72. Schäuble B, Cascino GD, Pollock BE, Gorman DA, Weigand S, Cohen-Gadol AA, et al. Seizure outcomes after stereotactic radiosurgery for cerebral arteriovenous malformations. *Neurology*. 2004;63:683–7.
73. Schuster L, Schenk E, Giesel F, Hauser T, Gerigk L, Zabel-Du-Bois A, et al. Changes in AVM angio-architecture and hemodynamics after stereotactic radiosurgery assessed by dynamic MRA and phase contrast flow assessments: a prospective follow-up study. *Eur Radiol*. 2011;21:1267–76.
74. Jiang P, Lv X, Wu Z, Li Y, Jiang C, Yang X, et al. Characteristics of brain arteriovenous malformations presenting with seizures without acute or remote hemorrhage. *Neuroradiol J*. 2011;24:886–8.
75. Shankar JJ, Menezes RJ, Pohlmann-Eden B, Wallace C, terBrugge K, Krings T. Angioarchitecture of brain AVM determines the presentation with seizures: proposed scoring system. *AJNR Am J Neuroradiol*. 2013;34:1028–34.
76. Turjman F, Massoud TF, Sayre JW, Viñuela F, Guglielmi G, Duckwiler G. Epilepsy associated with cerebral arteriovenous malformations: a multivariate analysis of angioarchitectural characteristics. *AJNR Am J Neuroradiol*. 1995;16:345–50.
77. Flickinger JC, Kondziolka D, Pollock BE, Maitz AH, Lunsford LD. Complications from arteriovenous malformation radiosurgery: multivariate analysis and risk modeling. *Int J Radiat Oncol Biol Phys*. 1997;38:485–90.
78. Park JC, Ahn JS, Kwon DH, Kwun BD. Growing organized hematomas following gamma knife radiosurgery for cerebral arteriovenous malformation: five cases of surgical excision. *J Korean Neurosurg Soc*. 2015;58:83–8.
79. Kim JW, Chung HT, Han MH, Kim DG, Paek SH. Brain edema after repeat gamma knife radiosurgery for a large arteriovenous malformation: A case report. *Exp Neurobiol*. 2016;25:191–6.
80. Flickinger JC, Kondziolka D, Lunsford LD, Pollock BE, Yamamoto M, Gorman DA, et al. A multi-institutional analysis of complication outcomes after arteriovenous malformation radiosurgery. *Int J Radiat Oncol Biol Phys*. 1999;44:67–74.
81. Inoue HK. Long-term results of Gamma Knife surgery for arteriovenous malformations: 10- to 15-year follow up in patients treated with lower doses. *J Neurosurg* 2006; 105 Suppl: 64–68.
82. Pan HC, Sheehan J, Stroila M, Steiner M, Steiner L. Late cyst formation following gamma knife surgery of arteriovenous malformations. *J Neurosurg* 2005; 102 Suppl: 124–127.
83. Yun JH, Kwon DH, Lee EJ, Lee DH, Ahn JS, Kwun BD. New nidus formation adjacent to the target site of an arteriovenous malformation treated by Gamma Knife surgery. *J Neurosurg* 2012; 117 Suppl: 120–125.
84. Di Betta E, Fariselli L, Bergantin A, Locatelli F, Del Vecchio A, Broggi S, et al. Evaluation of the peripheral dose in stereotactic radiotherapy and radiosurgery treatments. *Med Phys*. 2010;37:3587–94.
85. Cho YB, van Prooijen M, Jaffray DA, Islam MK. Verification of source and collimator configuration for gamma knife perfexion using panoramic imaging. *Med Phys*. 2010;37:1325–31.
86. Lawton MT, Kim H, McCulloch CE, Mikhak B, Young WL. A supplementary grading scale for selecting patients with brain arteriovenous malformations for surgery. *Neurosurgery*. 2010;66:702–13. discussion 713.
87. Wegner RE, Oysul K, Pollock BE, Sirin S, Kondziolka D, Niranjana A, et al. A modified radiosurgery-based arteriovenous malformation grading scale and its correlation with outcomes. *Int J Radiat Oncol Biol Phys*. 2011;79:1147–50.
88. Tang OY, Bajaj AI, Zhao K, Liu JK. Patient frailty association with cerebral arteriovenous malformation microsurgical outcomes and development of custom risk stratification score: an analysis of 16,721 nationwide admissions. *Neurosurg Focus*. 2022;53:E14.
89. Murthy SB, Merkler AE, Omran SS, Gialdini G, Gusdon A, Hartley B, et al. Outcomes after intracerebral hemorrhage from arteriovenous malformations. *Neurology*. 2017;88:1882–8.
90. Kano H, Flickinger JC, Nakamura A, Jacobs RC, Tonetti DA, Lehecky C, et al. How to improve obliteration rates during volume-staged stereotactic radiosurgery for large arteriovenous malformations. *J Neurosurg*. 2019;130:1809–16.

Publisher's note

Springer Nature remains neutral with regard to jurisdictional claims in published maps and institutional affiliations.